2.9 Dynamical property of the Cosmic Lattice

Let consider domain of uniform Cosmic Lattice (CL) space, not disturbed by mass particles and external waves. The average node distance for such lattice is a constant. The factors, that could influence the dynamical property of the lattice are only two: the intrinsic gravitation and the internal energy. The latter will cause some oscillations of the lattice nodes. Such lattice obviously will have a proper resonance frequency. This frequency will be determined by the mean distance between the neighbouring nodes and the average value of the intrinsic gravitation between them. We can consider, that in a steady state, the nodes will oscillate with their proper resonance frequency, that for uniform lattice will be a constant: $\nu_R = const$.

Let find out, how the motion of the node prism contributes to the inertial factor of the lattice. For this purpose we will use the twisted prisms model presentation of the real prisms (in the real prisms the twisted component of IG field is inside the whole volume of the prisms, due to its lower level structure, this is discussed in Chapter 12, Cosmology). The average velocity contribution from the axial oscillations from the central part of the twisted prism (inscribed cylindrical part of the prism) will be eliminated according to the conclusion 2.4.1.in §2.4.1. This will cause elimination of the first term in Eq. (2.7). The prism rotation although will contribute to the inertial factor caused by the IG interactions from the twisted peripheral part. The angular momentum from this rotation is:

$$L = m_{per}\upsilon_{per}r_{per} \qquad (2.11)$$

where: m_{per} is the intrinsic mass of peripheral part of the prisms (averaged value for left and right handed prisms)

υ_{per} is a peripheral velocity

r_{per} is a peripheral equivalent radius

The angular momentum divided by the rotational period of the prism t_p gives the work that determines the interaction energy. Substituting Eq. (2.11) in Eq. (2.7) we get the inertial factor I_F:

$$I_F = \frac{L/t_p}{E_g} = \left[\frac{m_{per}\upsilon_{per}r_{per}}{E_g}\right]f_p \qquad (2.12)$$

where: E_g - is the IG energy, that is constant for a steady state CL space

Let accepting that the velocity of the peripheral part of the prism has an upper limit value: $\upsilon_{per} = \upsilon_{lim}$. But this velocity and the prism rotational frequency f_p are connected. Then f_p will have upper limit constant value f_{lim}. **It is equivalent to say that the prisms in the lattice have upper limit of their angular frequency**. The latter could be defined by the intrinsic time constant of the intrinsic matter, (mentioned in §2.3), the prism shape factor and the distances between neighbouring prisms. So if the peripheral velocity has a limit, the inertial factor also will have an upper constant value, according to Eq. (2.12). The inertial factor of the twisted part is a predominant. Consequently it will define the interaction energy. **Then the limited value of the angular frequency will determine the finite value of the node resonance frequency.**

Conditions for stable lattice in empty space without boundary:

According to the stability rule, formulated in §2.6, the return forces should be conservative for any axis passing through the equivalent geometrical point. They should return the displaced node in a range of stable positions. The stable positions may not coincide with the geometrical equilibrium point. From the energetic point of view, the stable lattice should have point with low potential. Only stable gravitational lattices could really exist.

In the simplified model of twisted prism we admitted that they have a freedom of axial rotation within the CL node assembly influencing in this way each other. This is convenient for simplifying of the analysis. In reality, a rotation of the real prisms combined in CL node or any other gravitational lattice is not necessary. In the real prisms the internal modes of the IG field are in fact in rotational interactions. They are pure energy rotational modes, discussed in Chapter 12 (Cosmology) and they namely provide the twisted IG component of the IG field of the prisms.

2.9.1 Node configuration of CL structure

Fig. 2.20 illustrates a geometry of a single node in position of geometrical equilibrium, and the axes of symmetry.

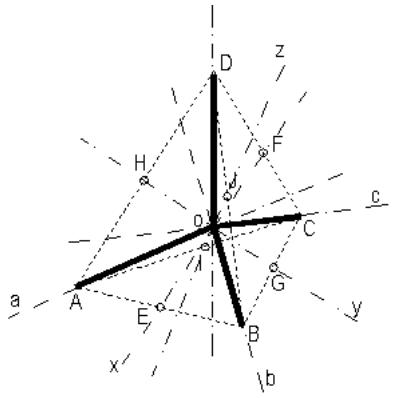

Fig. 2.20
CL node in geometrical equilibrium position
The two sets of axes of symmetry are: *abcd* and *xyz*

The thicker lines designate the four prisms of the node, each one at angle of 109.5 deg from the others. The ends ABCD forms a tetrahedron ABCD. The four axes, at which the prisms are aligned are **a, b, c, d,.** But the node has also another three axes of symmetry **x, y, z**, which passes through the middle of tetrahedron edges. This axes **x, y, z** are orthogonal each other. The **x,y,z** axes intercept the axes of **a,b,c,d** at **54.75 deg.**

If we not take into account the twisted part of the prisms, the x, y, z component does not have + and - direction. If taking into account only the twisted parts, the same axes may get + or - depending of the direction of the spin vector.

2.9.1.1Conditions for a stable lattice existence.

Analysing the return forces of cosmic lattice, according to the stability rule, formulated in §2.6, it is found that:

- applying gravitational law proportional to inverse power of two (for distance) leads to unstable lattice along the axes a,b,c,d.

- **applying gravitational law, proportional to inverse power of three leads to a stable lattice along a,b,c,d.**

- the return forces along x,y,z axes has valley symmetrical in respect to the geometrical equilibrium.

The return force of a single node of CL along the axes x,y,z is derived, by considering that the neighbouring nodes are in fixed position. For a node distance of few prism lengths, we may accept, that the centre of mass is always in the node centre. Then the return force, normalized to the product $G_o m_n^2$ is expressed by Eq. (2.14).

$$F = 2\left[\frac{x + d\cos\left(\frac{\theta}{2}\right)}{\left[x^2 + d^2 + 2xd\cos\left(\frac{\theta}{2}\right)\right]^2} - \frac{d\sqrt{0.5(1+\cos(\theta))} - x}{\left[x^2 + d^2 - 2xd\cos\left(\frac{\theta}{2}\right)\right]^2}\right] \tag{2.14}$$

where: G_o - is intrinsic gravitational constant; m_n - is the node intrinsic mass (equivalent mass for left and right handed node); d - is the distance between neighbouring nodes of CL, θ - is the angle between prisms axes in geometrical equilibrium.

The plot of equation (2.14) is shown in Fig. 2.21, where the displacement is normalized to d, and $d = 1$ is used.

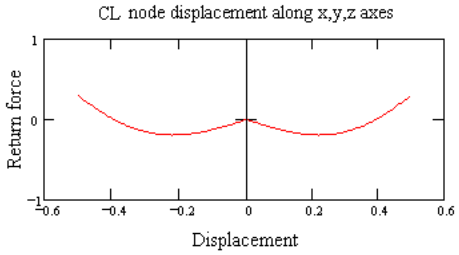

Fig. 2.21
Return force for displacement along x, y, z axes

The return forces plot shows, that two stable points exist along x,y,z axes, at both sides of the geometrical equilibrium point 0.

Let investigate now the return forces along a,b,c,d axes. The node geometry for displacement along a,b,c,d axes is shown in Fig. 2.22. The prisms

in the geometrical equilibrium are shown black, while for a displaced node they are shown grey.,

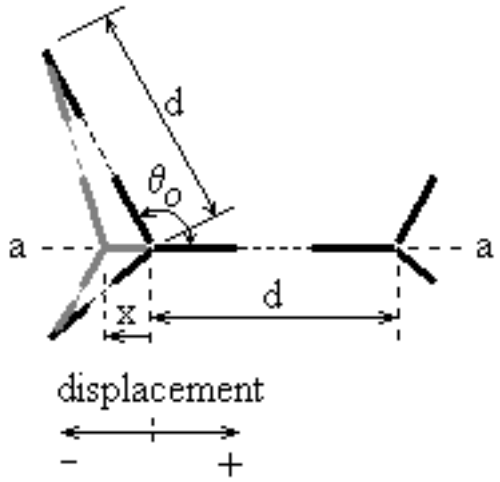

Fig. 2.22
CL node displacement along *abcd* axis

If not taking into account the node geometry and centre of mass change for small displacement, the return force for left displacement according to Fig. 2.22 is given by Eq. (2.15), while for right displacement - by Eq. (2.16).

$$F = \frac{1}{(d+x)^3} + \frac{3(x + d\cos(\theta_0))}{(d^2 + x^2 + 2dx\cos(\theta_0))^2} \qquad (2.15)$$

$$F = \frac{3(x - d\cos(\theta_0))}{(d^2 + x^2 - 2dx\cos(\theta_0))^2} - \frac{1}{(d-x)^3} \qquad (2.16)$$

The plot of the return forces for left and right displacements is shown in Fig. 2.23. The displacement is normalized again to d.

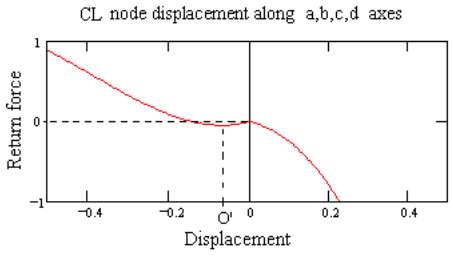

Fig. 2.23
Return force for displacement along a, b, c, d axes

The return forces along the axes a,b,c,d, does not appear symmetrical in respect to the geometrical equilibrium. It is evident from the plot, that the reaction forces for left and right displacement are quite different. Although, a valley exists in the left side of the geometrical centre 0, corresponding to point O'. This valley denotes a stable point for motion along a,b,c,d axes.

If investigating the motion in the intermediate axes we will see, that it is also stable. Then the CL lattice can be considered a stable without boundary holding conditions.

The valley shown in Fig. 2.23 was obtained, when applying IG force proportional to inverse power of 3. If applying inverse power of 2, the valley along a,b,c,d axes is missing. Consequently a Cosmic type of lattice is not possible if IG force is proportional to inverse power of 2. This result is in agreement with the accepted inverse power of 3 for IG force in empty space.

Despite disregarding the slight node geometry and centre of mass change, the simple equations (2.15) and (2.16) demonstrate the valley existence along a,b,c,d axes. In order to investigate more accurately the return forces and stiffness along the different axes, the two mentioned features has been also considered . In this case the equations are pretty long and will be not given here, but their plots are similar. For derivation of this equations the following considerations are made:

- the movable node is regarded as a group of four prisms, attached in their common end and always aligned to the neighbouring nodes, that are considered fixed;

- the forces between any one of neighbouring nodes and the centre of mass of anyone of the node prisms are applied;

- the centre of mass correction is applied

The centre of mass of the prism, presented as a mass bar depends of both - the distance and the angle. This dependence for inverse power of three low is larger than for the inverse power of two. Besides the long equations, some small corrections require graphical solving, fitting and iterations. The problem solving was focused on this displacement along a,b,c,d axes, for which a stable zone exists.

Fig. 2.24 shows a plot of return forces along the stable zone in a,b,c,d and x,y,z axes when the above mentioned factors are considered..

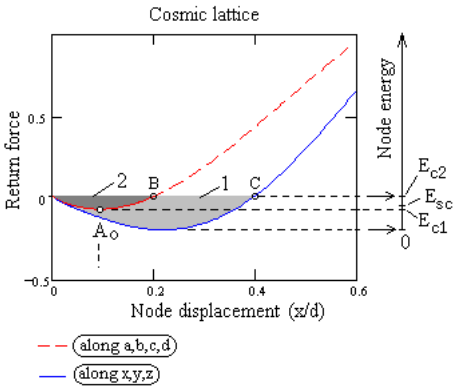

Fig. 2.24
Node energy diagram for cosmic lattice

The left scale shows return forces referenced to the geometrical equilibrium point of the node. But this is not a point of gravitational equilibrium. The gravitational equilibrium in fact is a three dimensional surface, centred around the geometrical equilibrium point. For displacements along intermediate axes, not coinciding with the two axes set, the valley will have different height. In the right side of the plot an energy scale for estimation of the node energy is shown. The energy scale is for reference only and is not proportional. The following energy levels are defined:

0 - is a zero level corresponding to the bottom of the valley, but from displacement in all possible directions, multiplied by the probability to vibrate in these directions.

E_{1c} - is the first critical level corresponding to the zero level for motion along and around the a,b,c,d axes.

E_{2c} is the second critical level. Energy above this level will lead to node destruction, because this is upper point for displacement along a,b,c,d axes (see Fig. 2.23). E_{2c} determines the full energy well of the CL node (maximum energy). It is equal to the sum of two energy wells, artificially separated and annotated in the figure, by 1 and 2. The energy well 1 is contributed by x,y,z axes and is much larger than the energy well 2.

E_{sc} is the superconductivity critical level. It will be discussed later.

The energy levels are very important features of the cosmic lattice. While the importance of E_{2c} is evident, the role of E_{c1} and E_{sc} are not so evident in a first gland, but it is very important for the EM field propagation and play important role for understanding the superconductivity state of the matter.

The full energy well is contributed mainly by the light gray area, but taken from a solid angle around x,y,z axes. The dark grey area 2 contributes to the node energy only above the level E_{c1}. The energy quantity (E_{c2} - E_{c1}) is a small fraction of the node energy well**,** because it is contributed only of small solid angle around 4 axes (instead of 6) and with smaller deepness.

It is evident also, that the stiffness for displacements along x, y, z axes is much lower that the stiffness along a, b, c, d axes.

Fig. 2.25. shows the return forces in a,b,c,d displacement, normalized to forces in x,y,z for two node distances.

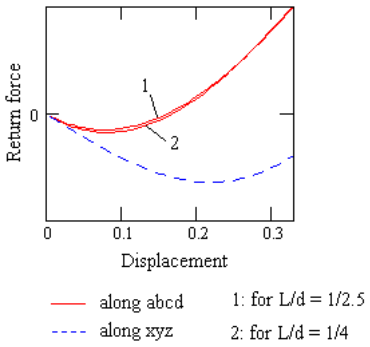

Fig. 2.25.
Return forces in case of node distance change

From the plot of the return forces in Fig. 2.25 one can make conclusion, that the energy ratio of {(node well)/(E_{c2}-E_{c1})} is slightly affected when the node spacing is changed. This is due to the finite dimensions of the prisms.

Analysing the return forces and stiffness for displacement along the both set of axes and all possible axes between them, it is obvious that the node will be able to vibrate in a complex way. It will be able also to store a kinetic energy due to its energy well. **This is the zero point energy (ZPE) of the**

node. The ZPE of the CL is mostly contributed by the valley deepness for x,y,z displacement, because it is symmetrical and deeper than the valley in a.b.c,d displacement.

Let to analyse the node oscillation for two cases:

A case: The node energy is between zero and E_{c1}.

2.9.2 Node oscillations described by vectors

The dynamical properties of the lattice could be studied by the analysis of the single node dynamics and the dynamical interactions between the nodes. This process is very complicated, but it can be simplified, if proper vectors are introduced.

The stiffness along the x,y,z axes is smaller than along a,b,c,d axes. The nodes tend to oscillate between the opposite valleys of x,y,z, but the trace curve could not be flat. The trace of oscillating node will not pass through the geometrical point O. It will bypass it, because the stiffness in the vicinity of this point is higher. The trace is a three dimensional curve, but its projection on a plane *xy* is shown in Fig. 2.26.

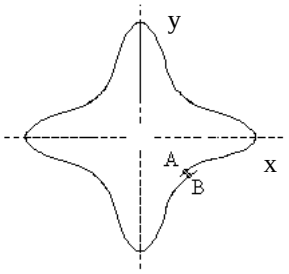

Fig. 2.26
Trace curve of the resonance cycle of the oscillating CL node

The trace curve of a single cycle will not pass also through the same initial point, as shown in the projection curve. Despite of this we can formulate a period between points A and B. **The trace period is a time between two adjacent traces, at arbitrary chosen closest points.** This period determines the CL node **resonance frequency**. The node inertial factor is very small, so the **resonance frequency is to be very high.** The nodes of lattice domain with constant node distance will have a constant resonance frequencies.

If considering consecutive periods, the node trace curve will not pass through the same point traces. For multiple periods, the trace will circumscribe a three dimensional surface. This surface will have a shape of deformed sphere with six bumps along x,y,z axes, and four deeps along a,b,c,d axes. We can call this surface a node trace quasisphere.

In any moments, the node have intrinsic inertial momentums with directions coinciding with the instant velocity vector. If integrating this momentums per one resonance period, we get node average momentum, that could be expressed also by vector, but passing through the geometrical equilibrium point of the node. We can call this vector a **node resonance momentum vector**, or abbreviated: NRM. It is more convenient to operate with such vector, normalized to its maximum value.

The node resonance momentum is a three dimensional vector, expressing the integrated intrinsic inertial momentum of the node for one period of the resonance oscillations. The origin of the vector is at the geometrical equilibrium point of the node.

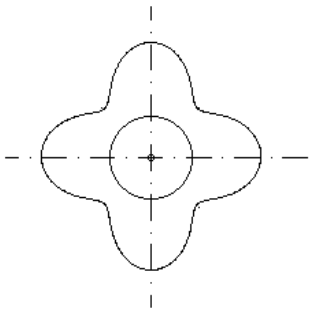

Analysing the node resonance momentum behaviour for large number of consecutive cycles, we will find that it has larger density in a cone along x,y,z axes, than along a,b,c,d axes. Then we can introduce the node density momentum vector.

The node density momentum vector is a product of the node momentum vector for many cycles multiplied by its differential angular cross section and average to its maximums at x,y,z axes.

The behaviour of the density momentum vector is described by a **node density momentum quasisphere.** It also have six bumps and four deeps, but their shape is not the same as the node trace quasisphere.

The shape of the density momentum quasisphere is shown in Fig. 2.27.

In order to investigate the features of the node quasispheres and introduce other vectors, a few en-

ergy dependent cases of the node oscillations will be analysed.

A. Case: The node energy is between zero and E_{c1}.

If considering a single node dynamics, a node momentum along a,b,c,d axes should not exist. However the influence of the neighbouring nodes will cause some small fluctuations along this axes. In a longer period of time, the node momentum vector will oscillate in a spherical coordinates, but spending more time around the x,y,z axes. The node quasispheres can be defined, for some large number of oscillations, but circumscribed in a random way. It will be still symmetrical, but the surface density could not be uniform.

B. Case: The node energy is between E_{c1} and E_{c2}. SPM mode of operation.

In comparison to the case A, the node stiffness near the axes a,b,c,d will be affected. In result of that, the node momentum vector will be affected by small force, tending to change the vector direction continuously. This will cause a precessional momentum, that will control the direction of node momentum vector in a definite way. In the same time the node momentum will flip from cone to cone around x,y,z, but more uniformly, than in case A. The consecutive cycles of the node momentums will define again quasisphere, but more systematically. The momentum vector for every consecutive cycle will be aligned in different directions, but with tendency of preserving the momentum of precession. In this case a **vector of precessional momentum** could be defined, whose period will contain a large number of node momentum periods. For one period of this vector, the node density momentum quasisphere will be completely defined. We can call this vector a **spatial precession momentum vector** or **SPM vector**, and the operational mode **SPM mode.**

The SPM vector is a spatial precession momentum of the node momentum oscillations.

In SPM mode of operation the node density momentum quasisphere is completely defined for one period of SPM vector.

If a gradient of gravitational or other field exists across the CL space domain, the node equilibrium may be biased, so for correct SPM mode of operation the node energy should be little bit above E_{c1}.

We could accept now, and prove later, that the CL node in normal conditions (superconductivity is excluded) has a capability to accumulate and preserve the full well node energy. This is the nominal ZPE of the vacuum. It will be shown in Chapter 7, that the relict radiation is manifestation of the ZPE of the CL space (BSM interpretation).

The node resonance and SPM frequency are related by the expression:

$$\nu_R = N_{RQ}\nu_{spm} \qquad (2.17)$$

where: ν_R - is the CL node resonance frequency

ν_{spm} - is the CL node SPM frequency

N_{RQ} - is the number of resonance cycle for one period of SPM

The coefficient N_R is a constant of the CL space and may have pretty large value. For now it is unknown, but some guess will be made in the next paragraphs. The accurate knowledge of this constant does not affects the results obtained by the BSM theory.

The SPM effect is essential feature of the lattice space. It helps to understand some basic properties of the space in which we live. These properties include: the quantum features of the space, the electrical and magnetic fields, the light velocity, the conductivity and superconductivity states of the matter.

2.9.3 Resonance frequency stabilization effect

The trace of the node is very complicated curve. Some quantitative analysis although could be done, in order to show that some stabilization effect of the resonance frequency exists. We may distinguish two stabilization mechanisms: weak and strong stabilization.

2.9.3.1 Weak stabilization mechanism

Let to consider two cases of CL node energies E_1 and E_2 lying in the range between the E_{sc} and the nominal ZPE level, as shown in Fig. 2.28.a.

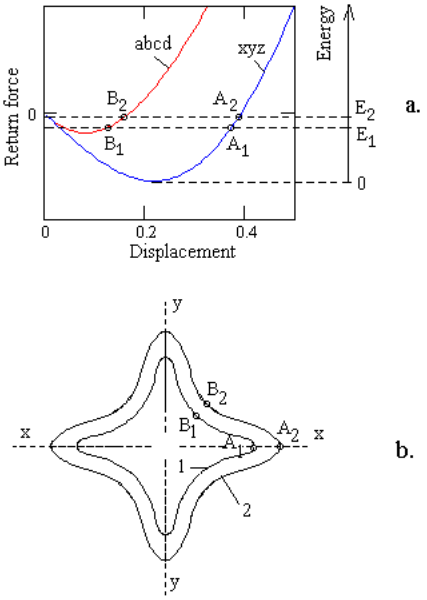

Fig. 2.28
NRM frequency stabilizing effect

Fig. 2.28.b. shows the projection of the trace of the node for one period of the resonance frequency. The projection is not of the classical type, but made in a way to preserve the path length and distance from the centre. Due to the centripetal acceleration the trace will tend to pass through the more distant points from the geometrical centre. For energy E_1 it will pass through the points A_1 and B_1, while for energy E_2 respectively through A_2 and B_2. Then the internal trace projection 1 will correspond to the lower energy E_1 and the external trace 2 to the higher energy E_2. The ratio between real traces lengths will be approximately preserved. The slop of return force in any point of the displacement curve gives the stiffness. From Fig. 2.28.b we see, that the return forces and stiffness for trace 2 are larger than for trace 1, and the stiffness of x,y,z curve is larger. Then the larger stiffness for trace curve 2 will tend to reduce the period. Consequently the change of the node stiffness of the two displacement curves exercises some kind of stabilization effect on the node resonance frequency. Therefore we may conclude that:

For CL node energies in the range between E_{sc} and nominal ZPE, a weak stabilization effect of the node resonance frequency exists.

2.9.3.2 Strong stabilization mechanism.

In the paragraph 2.11.3 the derivation of the light equation is provided. It will become evident, that the constancy of the light velocity is directly related to the resonance frequency. Then the resonance frequency should be stable in the same order that the constancy of the light velocity. Evidently a well defined and self regulated stabilization mechanism should exist.

One of the necessary condition for the strong stabilization mechanism is to work in conditions, where, the resonance frequency dependence of the ZPE is a continuous function. In this aspect the weak stabilization mechanisms fulfil this conditions. In the following analysis we will see, that the increase of the ZPE in the allowable limit, leads to a continuous increase of the resonance frequency.

Let analyse the frequency of not disturbed NRM quasisphere. In §2.10.3 we will see, that such nodes are associated with continuous fluctuations, forming a so called magnetic protodomains. In such aspect the nodes with not disturbed NRM quasispheres are simply referred as magnetic quasispheres (MQ). Let initially suppose, that the ZPE of the MQ is below the normal level. If it gets additional energy the oscillation amplitude and its frequency will get increase. But the amplitude increase may lead to overpassing the limit, corresponding to the E_{c2} level of ZPE (see Fig. 2.24). This could lead to destruction, but the CL has an ability to transfer the excess momentum to the neighbouring node. Due to the very small inertial factor of the node, the transfer of the excess momentum occurs for time less, than one resonance cycle. Consequently the average oscillating amplitude could not exceed the value corresponding of E_{c2}. In the same time, due to the zero point waves, (discussed later), every node has a possibility to support its nominal ZPE. This is confirmed by the background temperature of 2.72 K of the CL space. (A detailed discussion, calculation and comparison of this CL space parameter is presented in Chapter 5). Consequently the accuracy of the nominal ZPE determines the accuracy of the resonance frequen-

cy. There is a second factor, that also contributes to the stabilization. This is the mutual synchronisation of the MQ in result of their participation in magnetic protodomains. Consequently we may summarise, that:

- **The strong stabilizing mechanism of the CL resonance frequency is controlled by the two factors: the nominal ZPE of the node and the node participation in magnetic proto domains.**

Note: The magnetic protodomains will be discussed later. They are directly related with the permeability of the vacuum.

2.9.3.3 Analytical presentation of the frequency stabilization effect.

Here only a simple and aproximative analytical model will be presented. However it will give a basics for correct interpretation of the data from the Quantum Hall experiments in Chapter 4, from where the frequency stabilization effect becomes evident.

We will use two approaches, valid only for MQ node:

- node oscillations as a spring system
- node oscillations as an conical pendulum

A. Node oscillations model as a spring system

This option is only for a simple illustration without showing the strong stabilization mechanism. The resonance frequency is given by:

$$\nu_R = \frac{1}{2\pi}\sqrt{\frac{k}{m_n}} \qquad (2.17a)$$

where: k - is a stiffness, m_n is the node inertial mass.

In the QHE experiments we will see, that the node distance is unchanged, and we may consider, with a first approximation, that m_n is slowly dependent or almost a constant. We may determine the stiffness, by differentiating the return force along x,y,z axes (equation (2.14)) on the displacement, for a node distance normalised to unity. Then the stiffness is given by:

$$k = \frac{2}{A^2} - \frac{8\left(x + \cos^2\left(\frac{\theta}{2}\right)\right)}{A^3} + \frac{2}{B^2} + \frac{8C\left(x - \cos\left(\frac{\theta}{2}\right)\right)}{B^3} \qquad (2.17b)$$

$$A = x^2 + 1 + 2x\cos\left(\frac{\theta}{2}\right) \qquad B = x^2 + 1 - 2x\cos\left(\frac{\theta}{2}\right)$$

$$C = 8\left(\sqrt{0.5 + 0.5\cos(\theta)}\right) - x$$

Due to the reversible direction of the return force, the stiffness curve obtains a negative part, but this is artifact, due to the reference to the geometrical equilibrium point. To correct this we shift the curve up by the max negative value. Then substituting in (2.17a) and normalising to $(\sqrt{m_n})/2\pi$, we get the resonance frequency dependence of stiffness change.

$$\nu_R = \sqrt{k(x) + 1.33} \qquad (2.17c)$$

The plot of Eq. (2.17.c) is shown in Fig. 2.28.A. The node displacement *x* could be considered as a radius, corresponding to a lattice with defined stiffness.

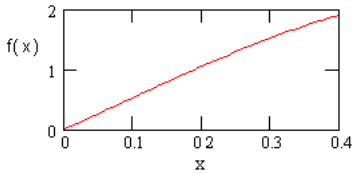

Fig. 2.28.A

B. Node oscillations model as a conical pendulum

In this case, the node oscillation properties, are simulated by a circular conical pendulum. The simulation is approximate and valid only for a MQ type of node. In this type of simulation the effect of the strong frequency stabilization will be shown.

The parameters of the circular conical pendulum (the trajectory is a circle) are shown in Fig. 2.28.B.

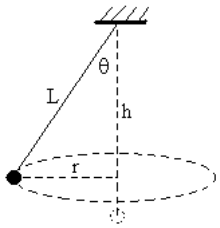

Fig. 2.28.B
Conical pendulum

We will associate the node displacement with the parameter *r* of the conical pendulum, the node distance - with *L* and the node energy - with the potential energy of the pendulum. Then for a uniform CL domain the oscillation period will depend only of the parameter *r*. The oscillation frequency of the conical pendulum is given by the equation

$$f = \frac{1}{2\pi}\sqrt{\frac{g}{h}} = [g[L^2 - r^2]^{-0.5}]^{0.5} \qquad (2.17.d)$$

We are interested of the node operation in the zone from the right side of point A_o, where the smallest trace curve radius is determined by the curve 2 and the larger radius from the curve 1. We may approximate the node trace curve with an equivalent circle, whose radius vary in the range between 0.23 to 0.29 of the node distance (see Fig. 2.24). Then the parameter r in eq. (2.17.d) will be substituted by $(x + 0.23)$, where *x* is the new argument that we may relate to the ZPE.

In order to simulate the loss of energy, when the node overpasses the ZPE level at large displacement, we will introduce a change of the *L* parameter of the pendulum. This change will begin when the argument *x* overpasses some threshold value. So we will define a continuous function with a kink. We may call this function an **energy dumping function**. For this purpose the following exponential function is used.

$$L(x) = \left[1 + 0.0106\exp\left[-\left[\frac{(x - 0.03)}{2.48\times10^{-4}}\right]^2\right]\right] \qquad (2.17.e)$$

The parameter L from Eq. (2.17.d) is substituted with L(x) of Eq. (2.17.e). In order to adjust the frequency span and frequency normalization to unity, we must select also a value for *g*, and offset the frequency *f* with some constant value. The final frequency simulation equation takes a form:

$$f = [22000[(L(x))^2 - (x - 0.23)^2]^{-0.5}]^{0.5} - 150.4 \qquad (2.17.f)$$

The energy dumping and frequency simulation curves are plotted respectively in Fig. 2.28.C a, b. The frequency stabilization is at $x = 0.06$. For the real conical pendulum model the dumping energy will stop to grow at the point of the stabilization, and **the frequency will get a fixed value**. For this reason the frequency down slop is shown as a dashed line. We see, that the stabilization effect is very sensitive to the energy dump. From the micro-scale point of view, the frequency uniformity between the CL nodes depends only of two factors:

- prisms uniformity
- node ZPE equalization

The high degree of prisms uniformity is accepted a priory, but its physical concept and analysis is presented in Chapter 12.

The second factor is self regulated by the zero point waves. The prove of this is the Cosmic background temperature uniformity.

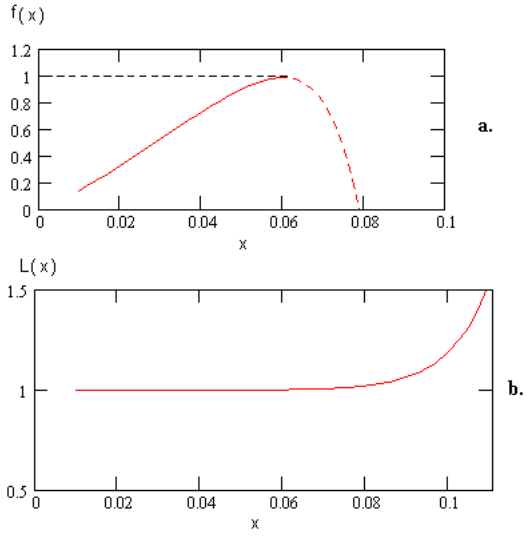

Fig. 2.28.C
Conical pendulum model for demonstration of the
resonance frequency stabilization

The demonstration of the stabilization effect here, does not take into account the appearance of the quantum stabilization process in CL space, and a possible change of the node inertial momentum for the range of *x* below the maximum. In the real case, the frequency dependence of the node displacement may not be so linear. The presented simple model, however, is helpful for interpretation of some results obtained by the Quantum Hall experiments (see Chapter 4.) In such aspect it helps to understand the dynamics of the CL node oscillations.

2.9.4 SPM vector affected by external electrical field

A. Case: The node energy is between E_{sc} and nominal ZPE

In a presence of external electrical field, the node resonance momentum vector will be affected by the vector of electrical field. The NRM will get preferential distribution along the filed. From one side, this will cause deformation of the node quasisphere, transforming it to prolate spheroid with bumps, aligned with the vector of electrical field. From a second side, the SPM frequency will be changed but the amount of this change will depend of the quasisphere deformation. In one of the next paragraphs, where the energy transfer is discussed, we will see, that the change is in direction of decrease the SPM frequency. While the NRM frequency is still stable, this means, that the SPM quasisphere is circumscribed by smaller number of resonance cycles.

The decrease of SPM frequency of node quasisphere in external electrical field is important feature of CL space.

The above mentioned feature helps to explain the electrical interactions between charge particles in CL space. This will be discussed later in this chapter.

The shape of the CL node quasisphere, affected by electrical field is shown in Fig. 2.29. The distance between the points could provide impression about the density of the node momentum vector in the particular direction

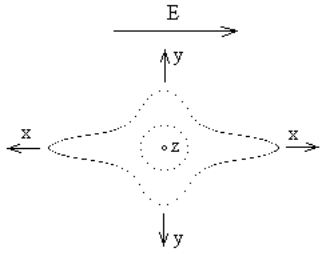

Fig. 2.29
Node density momentum
quasisphere affected by electrical field
E - direction of the field

B. Case: The node energy is below E_{c1}.

In this case the asymmetrical stiffness along a,b,c,d axes will be eliminated and will not control the node momentum vector. The external electrical field above some threshold level could be able to affect the vector, but random or controlled precession conditions do not exists. So a normal SPM effect here does not exist. The node momentum will define a node quasisphere, but severely deformed. The cross sectional momentum quasisphere will approach the shape of prolate spheroid with not so sharp bumps. Its shape is shown in Fig. 2.29.a.

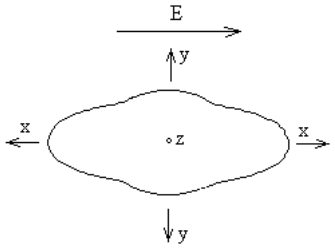

Fig. 2.29.a
Node density momentum quasisphere
in external electrical field
for node energy below E_{c1}

The deformed quasisphere will lead to increased propagation of the external electrical field in comparison to the case A. This is valid for subcritical node energy but not much below E_{c1}. For energy lower than some level, the propagation of the electrical field will start to decrease in result of a lack of node motion. In normal conditions, however, the CL lattice tend to keep its ZPE.

From the analysis of this case, it is apparent that:

- **In case of subcritical node energy a SPM effect does not exits**
- **The propagation of the electrical field in subcritical node energy is enhanced**
- **The magnetic field is not able to propagate in a lattice domain with subcritical node energy.**

The last statement will be proved in Chapter 4.

The three features cited above are important factors in the superconductivity state of the matter. They are discussed in Chapter 4.

2.9.5 SPM frequency for node energy between E_{c1} and E_{sc}

When the node energy is below E_{sc}, the slop of the return force along a,b,c,d is gradually, but significantly reduced in comparison to the slop of x,y,z force (see Fig. 2.24). This causes diminution of the SPM frequency stabilization effect, discussed in the §2.9.3. The change of stiffness along a,b,c,d below E_{sc} leads to decrease of SPM frequency even for the normal quasisphere (i. e. at absence of external electrical field). This effect plays important role in the superconductivity state of the matter.

Summary of introduced vectors and their presentation

- Node trace
- Node trace projection
- Node trace quasisphere
- **NRM** (node resonance momentum) vector
- **NDM** (node density momentum) vector
- SP (spatial precession) effect
- **SPM** (spatial precession momentum) vector

The **SPM** vector is obtained by the spatial precession effect applied on **NRM** vector. This could be expressed by the operator **SP**{}.

SP{NRM} => SPM

The control functions of the SP operator depend of the node energy conditions, discussed in the previous paragraphs.

The SPM vector can be presented by the following components and subcomponents as shown in Fig. 2.29.B.

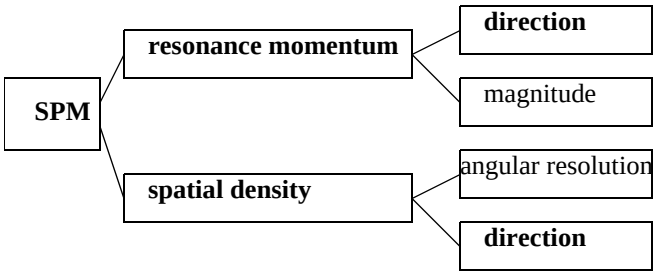

Fig. 2.29.B

The bold text is used for vector components, while the plane text is for the scalars. The node quasisphere is a convenient way for graphical presentation of the NDM or SPM behaviour. The SPM quasisphere is distinguished by the NDM only by its surface uniformity, due to the SPM effect. In the future analysis, where the conditions are implicitly known, the name node quasisphere will be used.

The quasisphere is a surface in spherical coordinates, circumscribed by a radius vector with components shown in the Fig. 2.29.C

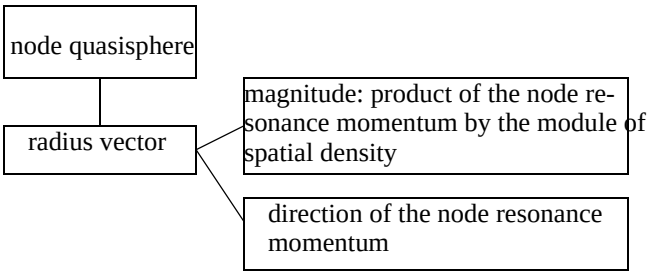

Fig. 2.29.C

2.9.6 Method of separation of intrinsic interaction processes contributed by the central or peripheral twisted part of the prisms.

When the interaction process in a lattice is analysed in a lowest level, the level of the twisted prisms, any interaction could be regarded as contribution of two prisms interactions: interaction due to the cylindrical core of the prism, and interaction due to the twisted peripheral part. The IG although could not distinguish the interaction between the cylindrical parts of right handed from left handed prisms. Then in stable lattice space, we could separate the interactions due to the cylindrical part of the prism from those due to the twisted part. A stable lattice space is this one, whose lattice, is in a steady state. There are processes of CL lattice destruction and rebuilding, where transition time phase exists (nuclear test explosion, for example). During such a process, the CL space is not in a steady state phase.

For IG interactions in which the cylindrical part of the prisms is involved, the following simplification could be applied.

- **From the point of view of the inertial factor, the IG interaction of the central part of the prisms of the opposite nodes are equivalent.**
- **For domain of stable lattice space, containing large number of nodes, the integrated result from the interactions between the cylindrical part of the prisms for one SPM cycle is equal to zero.**

The integrated result from the peripheral twisted part for prisms for one cycle of NRM or SPM, however, is not equal to zero.

- **IG interactions from the right handed and left handed prisms have different spatial momentum.**
- **The integrated results from interactions between the twisted part of the prisms in the neighbouring nodes of CL space are not equal to zero.**

We could apply the method of interaction separation in most of the cases related with the analysis of the electrical and magnetic fields. But when analysing the mass deficiency effect of the charged particles, for example, the interaction separation could not be applied.

In some other cases, like estimation of charges from extended helical structures, the symmetry of the lattice field beyond some critical radius should be checked.

We may apply the method of interaction separation for the NRM and SPM vectors. For this purpose we attach the following attributes to the vectors:

CP - standing for: **cylindrical part**

TP - standing for: **twisted part.**

Then the node vectors will have the following two components:

NRM(CP); NRM(TP);

SPM(CP); SPM(TP)

Some parameters of the CP and TP components of the vectors are equivalent, for example the period (frequency), the normalized quasispheres and so on. In the analysis, where this is implicitly understood, we can dismiss the attribute TP in the vector notation.

The method of interaction separation greatly facilitates the field analysis in a lattice space. It helps to provide definition and physical analysis of electrical charge, electrical field and magnetic field.

2.9.6.A Oscillating velocity distribution of the CL node

Let consider only a not disturbed CL space whose SMP quasisphere is symmetrical along xyz axes. For a given node distance, the quantum wells are filled and the zero point energy is a fixed parameter. We may assume that the acceleration is a linear. Then we may determine approximately the oscillating velocity distribution in the oscillating volume. In order to simplify the model, we may consider that the volume is equivalent sphere. Dividing this sphere in small unit volumes, we may estimate the instant velocity in each volume and build a histogram of the velocity distribution. The derivation of the expression giving the envelope of the histogram is quite long to be shown here, so only its plot is shown in Fig. 2.29.D

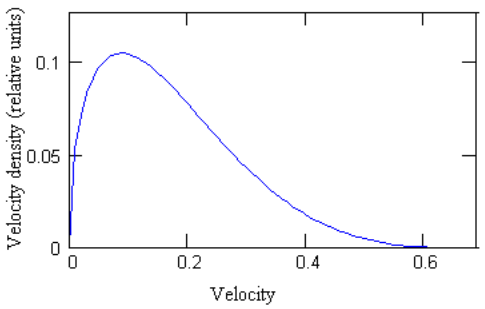

Fig. 2.29.D
Approximate shape of CL node velocity distribution in the oscillating volume

The velocity histogram is shown as a velocity density distribution in relative units. Despite the accepted simplification the obtained histogram approaches the shape of the distribution of population among the rotational states of the molecules. This feature will be additionally discussed in Chapter 9.

2.9.6.B Fine structure constant as one of basic features of the twisted prisms

The fine structure constant, denoted as α is one of very basic physical parameters. It appears everywhere from the quantum mechanics to any other theory. Its value is estimated experimentally with very high accuracy. In the BSM, it is also extensively used. In Chapter 10 theoretical equations for α are presented, allowing its determination with accuracy exceeding any observational value. One of the important conclusion of the BSM, is that α is an intrinsic common feature of both type of prisms. This feature will become apparent in Chapter 9, where the molecular oscillations are analysed. The final understanding of the fine structure

constant will become more apparent in the Chapter 12 (Cosmology), where the internal structure of the prisms, called a low level, will be discussed. For now we will show only some relations between CL space parameters in which α appears as embedded ratio.

The fine structure constant is dimensionsless. So it is a ratio of one and same type of parameters.

Let determine the amount of the gravitational energy, E, in empty space, between two equal prisms of same type at distance r_o. It is equal to the work done, when we separate them to infinity.

$$E = -\int_{r_o}^{\infty} G_{os}\frac{m_o^2}{r^3} = G_{os}\frac{m_o^2}{2r_o^2} = G_{os}\frac{\rho_o^2 V^2}{2r_o^2} \qquad (2.A.17.A)$$

where : m_o is the intrinsic mass, ρ_0 - is the intrinsic density and V the prism volume.

We may estimate the ratio of E for the central part and twisted part of the prism, as a ratio of their volumes quadratures:

$$E_{TP}/E_{CP} = V_{TP}^2/V_{CP}^2 \qquad (2.A17.B)$$

The twisted parts is this portion of the prism, that is left when removing the inscribed cylinder. If considering twisted prisms without spherical edges, the above shown ratio is a constant, that does not depend of the prism radius or length. It's value is 0.0105386. If considering, however, the two edges in shape of semispheres, the ratio E_{TP}/E_{CP}, becomes dependable of the length to radius ratio L/r (r - is the radius of the inscribed cylinder). For L/r ratio in the vicinity of 6.484, the energy ratio E_{TP}/E_{CP} becomes exactly equal to the fine structure constant $\alpha = 7.29735\times10^{-3}$. The corresponding L/r ratio, could not be accepted as real and seams to be a small. But we have to keep in mind, that the twisted prism is distinguished by the real twisted rods, mentioned in the beginning of Chapter 2. In the real twisted rods, the twisted effect is not so much external but internal feature of the intrinsic matter structure from which the prism is built. This will be discussed in the Chapter 12 (Cosmology).

When analysing the ratio of E_{TP}/E_{CP} in CL space, however, we have to take into account the feature, that the vectors IG(TP) and IG(CP) does not obtain equal propagation. The interaction involving IG(TP) vector propagates from right and left handed prisms, so the effect is additive, while those involving IG(CP) vector does not posses such feature.

If the E_{TP} energy, propagated in CL space from the right and left handed prisms is denoted respectively as $E^R_{IG(TP)}$ and $E^L_{IG(TP)}$, then the proper IG energy balance will be achieved at ratio:

$$\frac{E^R_{IG}(TP) + E^L_{IG}(TP)}{E_{IG}(CP)} = \frac{E_{IG}(TP)}{E_{IG}(CP)} = 2\alpha \qquad (2.A.17.C)$$

where: the energy $E_{IG(TP)}$ is just the energy related to twisted part (without referring to the right and left handed fractions), and $E_{IG}(CP) = E_{CP}$ is the energy related to the central part of the prism model.

The ratio given by Eq. (2.A.17.C), matches quite well with number of calculations, related with the electrical field, charge unity and atomic vibrations in the molecules. These problems are analysed in Chapter 9.

The fine structure constant shows its signature in many equations derived by BSM. It is related also with one basic parameter of the FOHS - the ratio between the confine radius and the second order helical step. So we may conclude:

- **The fine structure constant determines the ratio of the intrinsic energy transmitted by the twisted and the central part of the prisms. In CL space environment the right and left handed fractions contribute additively.**
- **The fine structure constant is exactly one and a same for both type of prisms**
- **The fine structure constant might carry a signature of the internal structure of the prisms.**

2.9.7 Summarized features of the cosmic lattice space

We can summarize the following features related to the dynamical property of the cosmic lattice.

- **The CL Space is able to handle intrinsic kinetic energy, that is the zero point energy of the vacuum. Its measurable parameter is the absolute temperature of the CL space**
- **The oscillating at resonance frequency CL nodes exhibit a spatial precession momentum (SPM) effect**
- **The rotation of the node resonance momentum is caused by the non symmetrical stiff-**

ness for node displacements along x,y,z and a,b,c,d axes.

- **The dynamical properties of the SPM vector are well characterised by the shape of the node quasisphere**
- **The vector SPM is directly involved in the unidirectional propagation of the photons**
- **The CL space can propagate two type of waves: quantum waves - involving equally mixed energy between the both type of nodes; and quasiparticle waves - involving not equally mixed energy**
- **The dynamical property of the gravitational lattice could be investigated more effectively if using the angular velocity as an argument against which the lattice parameters to be determined.**
- **The SPM effect helps to explain the quantum features of the space in which we live.**

2.9.8 Static and dynamical features of rectangular lattices

The rectangular lattices inside the helical structures are kept due to the concentric and radial configuration. They have much larger stiffness due to the larger prism density. They have symmetrical return forces. The valleys along the orthogonal axes at 54.7 deg relative to prisms axes are deeper. Consequently the oscillating node will exhibit also quasisphere behaviour, but with smaller bumps. The lack of asymmetrical return forces as for CL, however, means, that they not have stable precessional momentum. Consequently:

The rectangular lattice does not exhibit SPM effect and does not propagate a magnetic field. But it can propagate electrical field quite well.

The above mentioned feature is important factor in the trapping effect of the rectangular lattice in cylindrical space.

2.10 Disturbance of the lattice space around the helical structures.

2.10.1 Electrical charge and electrical field

The prism is extended solid object with anisotropic IG field aligned with the prism's axis. So the vector of aligned IG field according to the inverse cubic law is.

$$F_{ig} = G_o \frac{m_o^2}{|r|^4} \dot{r}$$

where: $\dot{r}$ is the directional unit vector.

If a huge number of prisms are ordered in some spatial configuration their effective component in CL space is also increased. If the prisms are of same type (right or left handed) the effective component also gets the same handedness. The internal twisted rectangular lattice [RL(T)] of the first FOHS are exactly such configuration. So the RL(T) is able to provide a strong modulation of the CL space. How this modulation affects the dynamical behaviour of the oscillating nodes?

Due to ZPE, the CL nodes oscillate with their resonance frequency that is much higher than the SPM frequency. Then the spin of the node prisms has also significant value. In §.. we will see, that in the absence of external disturbance (including for helical structure), the CL nodes are synchronized in protodomains at SPM frequency. When a FOHS is in such environment, a strong interaction appears between its RL(T) from one side and the mentioned above domains. While the ordered structure of RL(T) has a fixed spatial position, determined of the helical structure, the NRM and SPM phases of the mentioned above domains are free to be adjusted. In fact the phase of NRM vectors are adjusted to the RL(T) field due to a prism - to prism interaction. The domain synchronized at SPM frequency however increases the speed of the AC (alternative current type) type interaction.

The phase synchronization obtains also a spatial configuration, determined by the disturbance field of the RL(T). In result of this the CL node quasispheres obtain simultaneously elongation and spatial orientation. The node quasisphere obtains a shape shown in Fig. 2.29. The elongated shapes means, that larger number of resonance cycles are involved in the cones of elongated part of the quasisphere. The resonance cycle although is still stabilized. The kinetic energy of such quasisphere is larger, but SPM frequency is lower. There are two important features in this interaction process:

a) If one FOHS is inside of another external FOHS, the RL(T) of the external structure only modulates the external CL space

b) only the same type of node quasisphere are affected

The feature a) is explained by the lack of interface between the two internal RL(T), due to their different handedness. The referring to this feature is **equivalent to a rule, that the interaction handedness is determined by the external helical shell.**

The feature b) is a result of the parallel prisms interaction. In fact the opposite type node can get partially complimentary motion due to the induced interaction between the neighbouring nodes having different handedness

According to the above made considerations, we are able to provide the following definition of electrical charge and field:

(A) The electrical charge is a spatial region of CL space where the CL nodes obtains EQ type of node quasisphere arrange in particular order

(B) The electrical field is a CL space disturbance, that affects the spatial parameters of the NRM vector of CL nodes.

(C) The electrical charge elongates the nodes quasisphere, along its field lines.

(D) The electrical charge could be of static or dynamical type:

- (a)The static charge is invoked by one or group of helical structures whose charge is not compensated in proximity.

- (b)The dynamical charge is a quasiparticle wave or part of neutral wave propagated as a quasiparticle wave or quantum wave (photon). It appears as a spatial structure of running EQs.

It is evident, that in normal CL space, a static (not moving) charge is an attribute only of particles containing a matter. It is also evident, that in the higher order structures, containing FOHS, **only the external helical shell may exhibit electrical field.** This is the case of the structures shown in Fig. 2.10.b and Fig. 2.13.a.

Fig. 2.29.E shows the near filed electrical lines for the radial section of FOHS, whose internal RL(T) terminates by hole where another FOHS of opposite prism type has been., during the crystallization process.

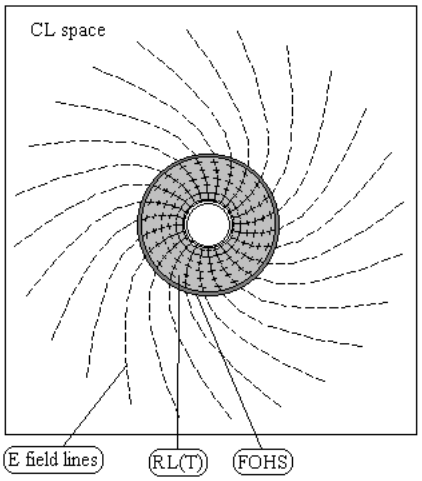

Fig. 2.29.E
Radial section of near E field of FOHS with internal RL(T)

The external filed lines follows the trend of the internal lines in the near field. In a far field of a static charge, however, they become radial, due to the Zero Point Waves that tries to equalise the ZPE of the CL nodes.

Some helical structures could exhibit near electrical field, but locked in space around the particle. The IG potential propagated the handedness (interaction due to twisted part of prism), must overcome some critical value, that depends of the neutral IG field of the helical structure (due to the cylindrical part of the prisms). Otherwise the handedness field will be locked by the neutral IG field. In this case, we can say, that the structure has a near field, but not a far field. The condition for "far" field may depend, also, of the overall geometrical shape of the helical structure, because different shapes can provide additional bending of the external near E field RL(T).

Stated in different words, a far electrical field is obtained, when the IG filed propagated the handedness, is able to escape from the local neutral IG field.

In this context, the structures shown in Fig. 2.11 and Fig. 2.14.a will have a near, but not a far electrical field. Although, when in motion, the structure of Fig. 2.14.a (neutron shape) can generate a weak magnetic field, and consequently, the near electrical field in this case becomes unlocked.

When the same structure is arranged in a configuration, shown in Fig. 14.b, it obtains a far electrical field even in a static position (proton shape), due to a spatial realignment of the lines of the near E field.

2.10.1.A. Graphical rule for a particle charge

In order to determine if the structure may have a far field for a lattice disturbance, we could apply the following graphical rule:

Draw tangent lines to every equidistant point of external FOHS of which the complex structure is made. Use equal line lengths larger than the size of the structure. If the endpoints of the lines are distributed not uniformly in a surface of sphere outside the structure, this helical structure will have far electrical field. If they are uniformly distributed, the structure will not have such field. Perform the checking procedure for a set of line with different lengths.

2.10.2 Interaction between particles, possessing a charge.

According to the definition of the previous paragraph we may use the term "charge particle" instead of helical structure possessing a FOHS with RL(T). A single charge particle elongates the quasispheres of the CL nodes of same handedness and align them to the vector of electrical field, due to IG field, propagating the handedness. The shape of distorted quasisphere was shown in Fig. 2.29.a. In the same time the electrical field decreases the SPM frequency of affected nodes.

Due to the handedness attribute of the particle's FOHSs and the CL nodes the right handed type of interactions are distinguished from the left handed type. We may consider that the interaction between FOHS IG(TP) field, from one side and the same type nodes, from the other is based on a prism to prism interactions (see §2.5). These type of interaction between the enhanced field from RL(TP) of the FOHS and the CL space, however, is quite stronger in comparison to prism to prism interactions in empty space.

The IG field of the charge particle could be regarded as a global synchronization field for every node. **In this case every node could be considered as oscillator, whose frequency is adjusted to the global IG(TP) field with the same handedness, provided by the charge particle.** For simplicity, however, we will consider that the charge synchronizes the nodes. Or in other words, the charge synchronizes the node momentum vectors of the same type nodes. This case is schematically shown in Fig. 2.30.a., where a rectangular lattice is shown for simplicity.

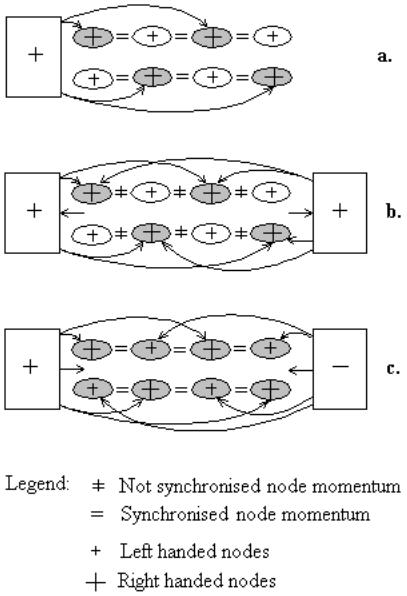

Fig. 2.30 Interactions between charge particles in lattice space

Fig. 2.30.b illustrates the nodes behaviour between two charges with a same handiness (polarity). In this case, the nodes are influenced by two global fields, generated by the two charges and they are confused from which field to get synchronization at the resonance frequency. In such way the node momentum vectors are almost aligned in the direction of the external field but their phases are not synchronized. Considering only the TP component of the node momentum vectors, the random phases will bump and provide forces of repulsion. This forces will push the charges away. The pushing force is active even if the charges are in motion with opposite direction. This is possible, because, the passed nodes gets readiness quite fast, due to their small inertial factor.

Fig. 2.30.c illustrates the node behaviour between two charges of opposite polarity. In this case every node get synchronization from the global field corresponding to its polarity (handedness). There is not conflict of synchronization. The positive nodes gets node momentum synchronization

provided by the positive charge, and the negative nodes - by the negative charge. The both charges although are not synchronized between themselves. How the node momentum phase can be adjusted in order all the node to be in phase and to get attraction force? The explanation is the following:

The propagated TP NRM reaches the more distant nodes of same type with some delay (determined by the light velocity), but the phase differences between the neighbouring opposite nodes will have some stable value. This constant phase difference could be eliminated, by suitable displacement of the nodes from their geometrical equilibrium points. In result of this, the node momentums of all the nodes appear synchronized and the charges get attractive force due to the IG(TP) attraction.

Let to analyse the dynamics of the attraction forces, when the opposite charge particles are in motion. The neighbouring quasispheres, are both synchronized by the external field. They eliminate the constant phase difference between themselves by proper geometrical displacement. Consequently the neighbouring nodes obtain absolutely complimentary motion. As a result of this, they tend to become closer, creating forces of attraction. The mean node distance although could not be changed, as will be seen from the photon propagation analysis. The attraction forces become applied to the external charges, that generate them. If the opposite charges are not fixed they will move under the attraction force. The motion, although could not diminish the attraction force effect, as the phase propagation of TP NRM is much faster, than the velocity of the moving charge particle.

In a similar way**,** it can be considered, that the CL space between same type of charges creates repulsion forces, applied to the charges.

In a case of single charge, the opposing interactions of the opposite nodes are missing, because they do not have spatial reference point in order to resist.

Summary:

- **The sign of the electrical charge is determined by the handedness of the prism, from which the external shell facing the lattice space is built.**
- **Internal helical structure (shell) can be considered as a hidden electrical charge, while it is completely inside of another helical structure. Once it appears in open CL space, its charge also appears.**
- **The charge particles are able to interact between themselves due to the ZPE of the lattice nodes.**
- **The attractive and repulsive electrical forces are reactions of the CL space, applied to the charge particles**
- **Electric and magnetic interactions are impossible at lattice temperature of absolute zero.**

If a finite amount of atomic matter in some particular conditions is at temperature of absolute zero, it does not mean, that the surrounding CL space is at the same temperature. The ZPE in open space is equalized very rapidly due to the Zero order waves

2.10.3. Node quasisphere behaviour in a permanent magnetic field

Let consider CL domain away from any static or dynamic electrical charge. The common synchronization of the CL nodes in this domain require finite time. We may accept apriory that this time is larger than the resonance period of CL node. This will become apparent later. Having in mind also, that the EQ CL has a larger energy than MQ node we may conclude:

In not disturbed CL space the CL nodes can not get spontaneous EQ synchronised at the resonance frequency because this will means a spontaneous creation of electrical charge.

Let investigate the possibility for spontaneously synchronized normal quasispheres nodes in not disturbed CL space domain but at SPM frequency, that is much lower than the resonance one.

In order to propagate an external magnetic field, the CL node energy should be above the E_{sc} level. In this case every node exhibits stabilized resonance and SPM frequency. Analysing the node fluctuations in this energy conditions, we find two antagonistic processes:

1) The system try to keep uniformity energy level

2) The system try to keep the lowest state by minimizing the interaction energy between the nodes.

From the point of view of the neighbouring node interaction, the lower interaction energy corresponds to commonly synchronised nodes. This is illustrated in Fig. 2.31 in two dimensions, but it is valid for three dimensional space, as well. In a result of this effect, it is very probable, that CL may contain commonly synchronized domains comprising of large number of nodes. Any such domain will exhibit a common SPM field, that is a features of magnetic field, if they are connected in close contour. So the field of this domains has a feature of local magnetic field, but with open lines. If their lines recombine in closed magnetic line, an energy will start to circulate and this will change the CL energy uniformity. For this reason the mentioned magnetic protodomains, continuously fluctuate and recombine the mutual node synchronization. When an external disturbance with the same SPM frequency is applied, the magnetic protodomains readily accept this synchronization and organize themselves in loops, that become closed in the CL space. Depending of the strength of the external field it may pump the ZPE energy of the nodes. The mutual synchronization of the magnetic protodomains, that become part of the magnetic field lines is illustrated in Fig. 2.31.

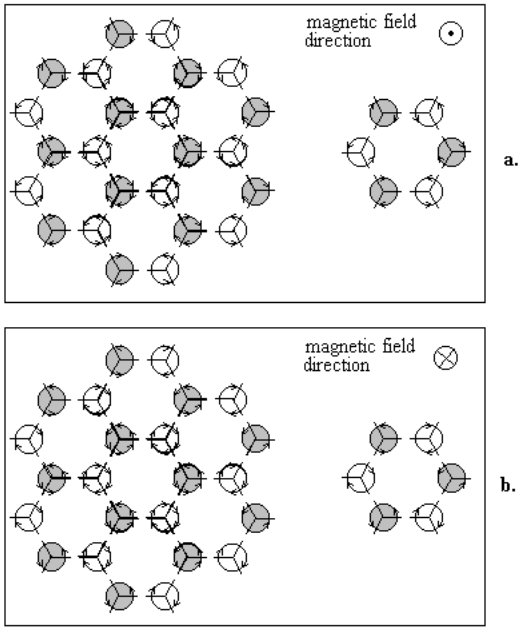

Fig. 2.31
Magnetic protodomains in CL space

The figure shows, the two type of nodes in one projection plane. The arrows show the confinement between the direction of the SPM vectors of the neighbouring nodes. Their directions are confined in a three dimensional space, but with one very important detail. The phase between same type of nodes is zero, but between the different type of nodes is equal to $\pi/2$. In result of this a wave motion is possible in two opposite directions, as shown in Fig. 2.31.A. These two directions in fact define the direction of the vector magnetic field.

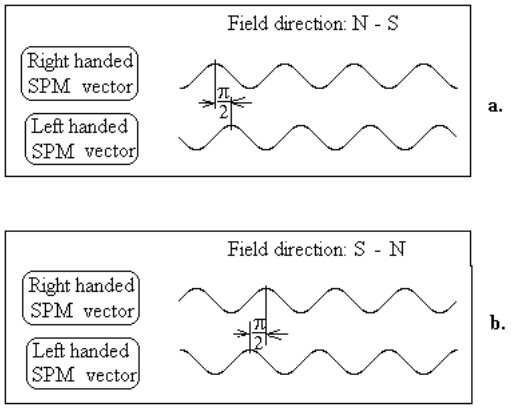

Fig. 2.31.A
Direction of the magnetic field vector, defined by the phase difference between the SPM vectors of both type of nodes

If analysing the interaction energy transfer between the nodes, we could find, that some portion of energy really circulate in the closed magnetic line. If this line is intercepted by a conductor, the circulated energy dissipates in it in a form of induced electrical field, pumping the nodes of the conductor space. If the conductor is a closed loop an electrical current is generated.

If the node quasispheres are distorted by electrical filed, their directional property will be disturbed and the spatial synchronization between the neighbouring nodes will be also disturbed. If the condition for the phase difference of $\pi/2$ has some tolerance, the distorted quasisphere also will have some critical value, beyond which the magnetic filed propagation is not possible.

The existence of magnetic protodomains may explain the magnetic constant of CL space, known as a permeability of the free space μ_o.

The rectangular lattices does not have a frequency stabilised SPM effect, and consequently, could not propagate magnetic field.

Knowing the property of the not distorted and distorted quasisphere of the SPM vector, in the further analysis we may refer to them simply as electric and magnetic quasispheres. From this point of view it is convenient to introduce the following abbreviation:

EQ standing for **Electric Quasisphere**

MQ standing for **Magnetic (not disturbed) Quasisphere**

Summarizing the analysis, we can provide a definition of the magnetic field in CL space:

- **The permanent magnetic filed in CL space is composed of closed magnetic contours formed of magnetic field lines in which excess energy is circulated.**
- **The field line is formed of spatially aligned node domains, connected in closed loop. The SPM vectors of left and right handed nodes, along the magnetic line, are spatially synchronized, while the relative phase difference between them is equal to $\pi/2$.**
- **A node quasisphere, that is distorted beyond some point, could not be included in a magnetic line. Such distortion is an attribute of electrical field.**
- **The rectangular lattice inside the FOHS can't propagate a magnetic field.**

2.10.4 Quantum electromagnetic wave

2.10.4.1 Energy propagation between neighbouring nodes

In the return force analysis, the neighbouring nodes were considered fixed only for simplicity. In fact the oscillation of any one single node could not be isolated from its neighbour.

The dynamical model for this exchange is very complicated, although an aproximative analogy could be made with a system of elliptical conical pendulums, attached to a common spring. A configuration of such system is illustrated in Fig. 2.32.

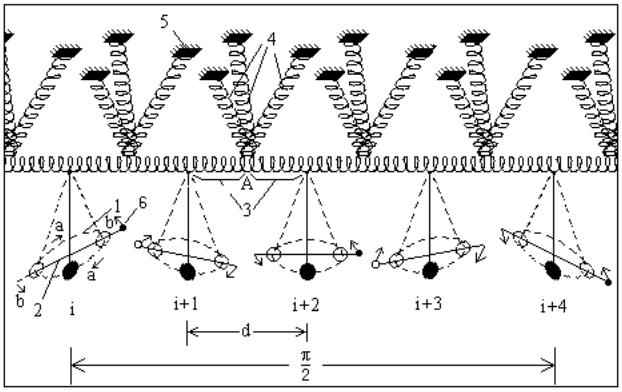

Fig. 2.32
System of conical pendulums in a common spring

The common spring is attached to fixed pads 5 by set of other strings 4 with equal lengths. The pendulums, having equal length and mass, are mounted equidistantly. All pendulums have one and a same oscillating frequency. Let to induce, in first, a conical oscillation of the left most, pendulum, but without precessional motion of the long axes 2. For enough long time interval, a steady process will occur and the neighbouring pendulums will get complimentary motion, also without precession. Let then invoke a continuous precession in the left most pendulum i, with direction shown by the arrows b-b. A continuous energy for the precessional motion of this pendulum could be supplied by a magnetic field below the pendulum mass. In result of spring stiffness the neighbouring node also will get such precession, but in opposite direction and with some delay. This precession will be propagated with delay to the next pendulums. The delay depends of the spring stiffness and lengths, from one side and the pendulum mass and length from the other. After many periods, we will find that the precession axes of (i+n) pendulum is in a same position as the pendulum i. Following the black reference point 6, we see that in our case the pendulum (i+4) gets delay of $\pi/4$. Then for this example we have n=16, and the precessional phase of the long axes will be repeated in distance nd. In the same time all pendulums will have one and a same

precessional period, but their phases will differ by a constant value. So a wave like motion of energy occurs with a spatial wavelength $\lambda = nd$.

The provided model could be used for better understanding the property of the CL in wave like energy propagation. The following analogy can be used:

Pendulum model		**CL node dynamics**
oscillating frequency	<=>	node resonance frequency
long axes momentum	<=>	NRM vector
long axes precession	<=>	SPM vector

When the lattice is in a steady state, it has only proto- magnetic domain fluctuations, whose energy is a part of its ZPE. In this case we may consider, that the energy is equally distributed between the both type of nodes. The amount of ZPE, although, could not pass the upper critical level Ec_{r2}, because this will lead to a lattice break. The CL, however, has ability to react fast enough: the excess energy of the node is propagated to the neighbouring node.

Let suppose that one node gets excess energy above E_{cr2}. We have to analyse the node motion during one resonance cycle. When moving in a destruction direction, the node will affect the four neighbouring nodes whose prisms are of opposite handedness. While the intrinsic interaction from the CP of NRM vector leads to node deviation toward the destruction a,b,c,d zones, the TP of NRM vector try to keep the node motion away from these zones. In result of this, the neighbouring nodes take part of the excess energy. This energy is then propagated to their neighbours in a same way. There are two node distances in CL lattice, considered as a neighbouring node distance: distance along a,b,c,d axes, and distance along x,y,z axes. The second one is about twice larger. Let to analyse the momentum transfer between two neighbouring (by x,y,z axes) nodes, as illustrated in Fig. 2.33.

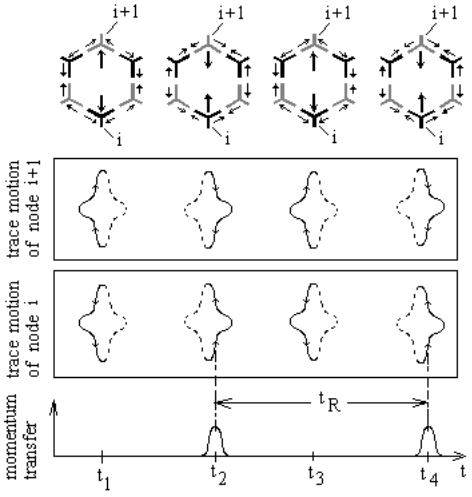

Fig. 2.33

Two neighbouring (by x,y,z axes) nodes (i) and (i+1)are shown in the upper part of the figure for four consecutive time moments. The motions as a part of resonance cycle are shown by arrows: the big arrows are for motions along x,y,z and small arrow - along a,b,c,d axes. The energy between (i) and (i+1) nodes is transferred through the two arms, formed of nodes. **While the arrow directions indicating the motion of the two arms are symmetrical, the prisms spin rotation due to prisms interaction are not symmetrical. This will reflect to the balance of the momentum.** The trace of motion and the momentum transfer are shown below. We see, that the momentum from node (i) transfers to node (i+1) in the position, when they are closer. The most important fact is that the condition for momentum transfer occurs ones per resonance cycle. Consequently we may accept that:

The excess energy in CL is propagated with velocity of one node distance along x,y,z axes per one cycle of NRM vector. The resonance cycle for the electrical quasisphere, however may be different, than the magnetic one.

The above rule is simply expressed by the equation:

$$\upsilon = d_{xyz}/t_R = d_{xyz}\nu_R \quad \text{(m/s)} \qquad (2.17.A)$$

where: d_{xyz} - is a node distance in x,y,z direction, t_r and ν_R - are respectively the resonance time and frequency for EQ.

According to the analysis of the previous paragraph, the nodes of the CL in steady state are connected in temporally magnetic protodomains with synchronized SPM vectors. This condition favours the start of wave energy propagation. In the steady state of wave propagation, the phase difference of the SPM vectors of neighbouring nodes is very small, and their quasispheres are aligned. So the propagation of the excess energy between the nodes is in a moment when their bumps are aligned, with a very small phase difference. In such conditions, the efficiency of the momentum transfer is maximal. Then we may conclude, that the propagated excess energy, will influence the phase of the SPM vector.

The excess energy is carried by the EQ nodes (electrical quasispheres) and is propagated with a speed of one node distance per resonance cycle. **It is more convenient to analyse the process of the energy propagation by considering a running EQ, instead of the stationary one**. The resonance frequency of the EQ nodes may be different than the MQ nodes and could depend of the EQ polarisation. The excess energy may involve a large, but finite number of running EQs. So in some point they have to contact with MQs, having different resonance frequency. In proper spatial configuration of the running EQs, the frequency difference between the EQs and MQs may be spatially distributed along a large number of EQs with gradually reduced polarization (eccentricity). This means that the major axis of the eccentricity between the neighbouring E's will have small spatial deviation. The MQs do not carry excess momentum. **Consequently:**

- **the spatial energy distribution should terminate with MQs.**

This condition is very important for the conservation of the excess energy in a finite volume. **It provides the boundary condition of the propagated wave.**

The boundary conditions are very important isolating factor. The above defined condition, however, is very restricted for quantum waves with different energies. The possible solution of this problem is the assumption, that the boundary condition could be any subharmonic of the SPM frequency. In such conditions the separation between the nodes involved in the wave propagation, from those, involved in the magnetic protodomains is optimal. This consideration become more evident, if we analysing the SPM vector behaviour of the stationary boundary nodes. Let define a reference point of the wavetrain, for example, when the E vector passes through its maximum in one fixed spatial point. We have to estimate the SPM vector of a stationary node residing in a plane passing through the above selected point and normal to the axis of the wavetrain but in distance corresponding to the boundary conditions. We have to estimate how many SPM cycles the boundary stationary node will pass between two consecutive maximums of the E vector. The results are given in the Table A.

Table 1: A

Subharmonic number	Wavelength	Number of SPM cycles of the boundary stationary node
1	λ_{SPM}	1
2	$2\lambda_{SPM}$	2
3	$3\lambda_{SPM}$	3
n	$n\lambda_{SPM}$	n

From the view point of the quantum wave, the boundary conditions are provided by the running MQs that are at the boundary, but from the side of the wavetrain volume. Their SPM vector is also a subharmonic of the SPM frequency. There is also a second condition for the quantum wave, that assures its integrity.

Consequently, the quantum wave is characterised by two basic conditions: boundary conditions and quantum wave integrity.

The two basic conditions can be formulated as:

- **Boundary conditions are provided of running MQs whose phase of propagating SPM vector is subharmonic of the SPM frequency.**

- **The integrity of the quantum wave is related with the synchronization conditions between the running quasispheres involved in the quantum wave volume.**

The integrity of the quantum wave will be discussed in the next paragraphs.

According to above considerations it appears, that the shortest quantum wave corresponds to SPM frequency. From the point of view of terminology consistency with the quantum waves, that are subharmonics, this quantum wave is often referenced as a first harmonic of SPM frequency. For the Earth local field its wavelength is equal to the Compton wavelength. This is the shortest wavelength generated by the electron system (discussed in Chapter 3) and defines the limit of the X spectrum. Periodical motions of helical structures in steady state CL space generate waves, whose frequencies are subharmonics of SPM frequency.

Here a question may arise about the gamma rays, that posses larger energies, than the X rays. This is discussed in one of the next paragraphs.

The SPM vectors behaviour of the nodes, involved in the energy propagation for first and second subharmonics are shown respectively in Fig. 2.34.a and b. The node quasispheres are shown by their envelopes. The circular shape corresponds to node quasispheres, whose SPM frequency are affected, but their shapes are not. The ellipse corresponds to quasispheres for which the both parameters: the SPM frequency and the quasisphere shape are both affected. The first one favours the magnetic-like field propagation, while the second one - the electrical.

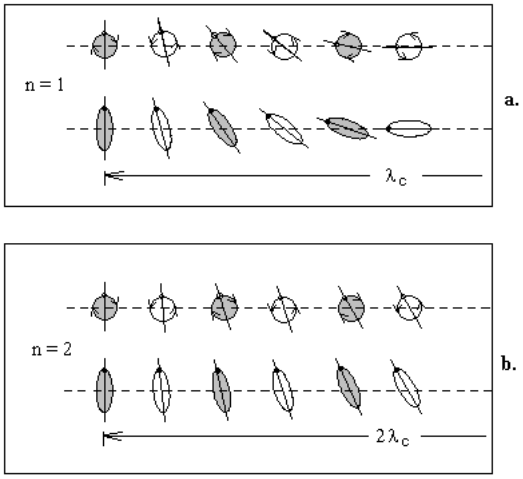

Fig. 2.34

The case **a.** shows fragment of a EM wave, in which the excess energy propagates in one direction at distance equal to the SPM wavelength for one period of SPM vector. In case **b.** the excess energy propagates in distance twice the SPM length, but for two periods of the external (not involved) nodes SPM frequency. In the second case, the SPM frequency of the participating nodes is twice lower.

In reality, the node quasisphere, involved in the wave motion, may have large range of distortions between sphere and prolate spheroid. Although, we could not expect, that they have a sharp transition between their possibility to propagate electrical or magnetic field. Some extended ranges with partial overlapping between them are more probable.

The above illustration, still does not uncover the full features of the quantum wave propagation, but put a light on it.

One particular feature of the neighbouring nodes, that are of opposite handedness is that, the coordinate system of their x,y,z axes are rotated at 90 degrees each other, but they are completely equivalent because they do not have (+) and (-) directional features. **So it appears that the x,y,z coordinates of all the nodes are aligned and their axes pass trough the bumps of the node quasispheres**. This fact leads to a guess that the EM waves propagate in directions determined by x,y,z

coordinates, but having in the same time rotational features caused by the a,b,c,d axial interactions (SPM effect). Then the induced wave will have a helical momentum. This momentum will keep the energy propagation in a straight direction. The EM waves are wavetrains with many repeatable cycles of SPM vector of the running quasispheres, involved in the wavetrain.

2.10.4.2 Quantum wave configuration.

The propagated wave occupies a region around the propagated axes with gradually but finite drop of the energy at given radius. Knowing that the vectors E and H are orthogonal each other in any moment, we can build configuration of the EM wave. It is easier in first to illustrate the node configuration for a standing wave, where the running nodes might be regarded as frozen in the time. Fig. 2.35 shows only the central parts of such waves fore two cases **a.** not polarized wave, and **b.** - polarized wave.

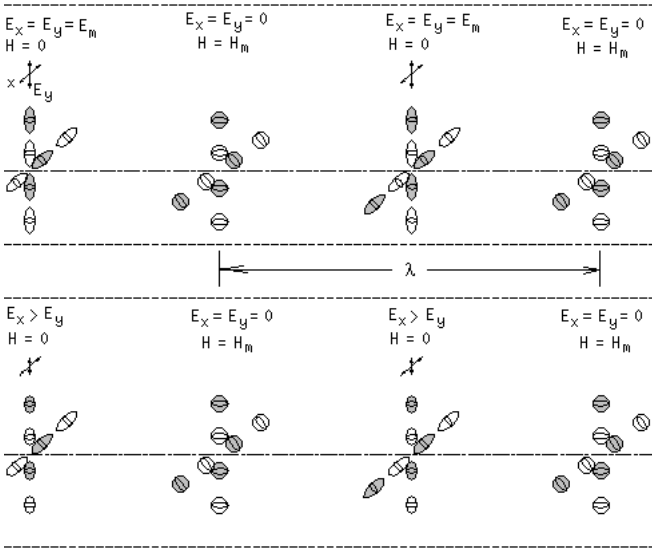

Fig. 2.35
Central part of standing quantum EM wave

The peripheral part of the quantum wave is not shown for simplicity. In order to satisfy the boundary conditions, the elongated shape of the quasispheres in a radial direction gradually transverses to a spherical one (EQs gradually transfer to MQs). The direction of wave propagation coincides with the horizontal axis. The spherical shapes in the standing nodes correspond to H_m. Their SPM frequencies although are subharmonics of the external not affected CL nodes, according to the quantum EM wave rule. The quasispheres between the standing wave nodes (do not confuse with the CL nodes) have intermediate distortions.

The configuration of CL nodes quasispheres in the central part of normal EM wave, frozen in time is illustrated in Fig. 2.36.

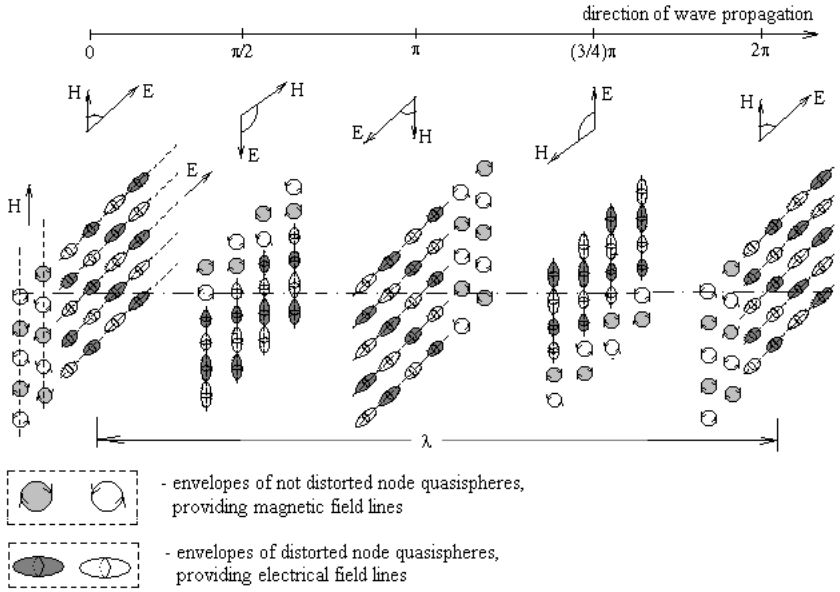

Fig. 2.36
CL node quasispheres for not polarized EM wave

The shown mutual positions of the node quasispheres, allows the vectors E and H to be perpendicular each other in all spatial points and for all time moments. Note that the left and right handed quasispheres are equally affected by the EM wave propagation. The radial extension of the EM wave is not shown in this figure. This type of EM wave in which the right and left handed nodes are equally polarised is a neutral quantum wave.

We see that the **node quasispheres affected only by frequency provides the magnetic field vector H, while the quasispheres affected by both: the frequency and the shape, provides the electric field vector E.** So the first type of quasisphere could be referred shortly as magnetic and the second type as electrical.

If following the trace of the magnetic quasispheres along the z axes according to the figure, we see that it circumscribes a helical trace. But we have to confirm that this is true. Let to consider two options: a) the magnetic quasispheres are aligned in a straight line along the axes z; b) the magnetic quasispheres are aligned in a helical curve centred along the z axes. The both cases are shown in Fig. 2.37.a and b. respectively, where 1 is a trace of the electrical quasispheres and 2- a trace of the magnetic quasispheres.

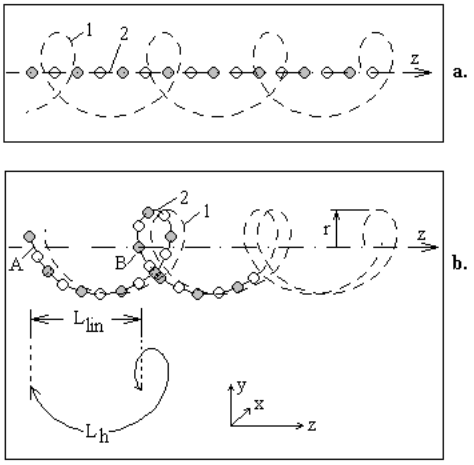

Fig. 2.37

In the steady state process of wave propagation, the neighbouring magnetic quasispheres should have enough time in order to combine in proper SPM phase difference, that will be much less than the SPM quasisphere bumps width. Then we may consider, that the PP (phase propagation) of NRM vector propagates through the maximum points of the bumps. The light velocity can be de-

termined by the ratio between the propagated distance for one SPM cycle, divided to the time of this cycle.

If considering that the magnetic quasispheres in EM wave have configuration shown in case **a**. of the figure, then the wave velocity will be completely determined by the parameters of the magnetic quasisphere only. But we know that the light velocity depends by both: the magnetic and dielectric property of the vacuum according to the equation:

$$c = \frac{1}{\sqrt{\mu_o \varepsilon_o}} \qquad (2.18)$$

where: μ_o is the permeability and ε_o is the permittivity of the vacuum.

The acceptance made above for case **a.** is in conflict with Eq. (2.18), so the case **b.** should be valid. In this case the electrical quasisphere will influence the curvelinear path L_h. However, it will affect also the linear direction, that is a direction of the wave propagation. **In other words the trace of any one magnetic quasisphere involved in the quantum EM wave, is a helix centred around the axis of the wave propagation.**

From the feature of the CL space in electrical field, we found, that the space between charge particle provides interaction force, and this effect is caused by the synchronized neighbouring quasispheres. But the arrangement of the electrical quasispheres in the photonic wave is completely similar. Consequently a same effect could be expected. In result of this the photonic wave, containing positive and negative quasispheres should exhibit also attractive Coulomb forces. The integrity of the photonic wave is due to this forces. This will be further discussed in the next paragraphs.

2.10.4.3 Boundary conditions of the quantum wave

Let consider now one very important feature of the photon propagation. A single photon can pass enormous distances in the Universe - billions light years without any energy loss. Evidently its energy loss is practically zero. How is this achieved? Obviously, the photon carry its energy in narrow space with diameter about its wavelength, that is perfectly isolated beyond some radius. (The classical wave function does not provide this feature of the photon).

The photon wavetrain contains equal number of electrical and magnetic quasispheres. The magnetic quasispheres are not connecting in a loop like in a permanent magnetic field. Consequently the magnetic quasispheres could not carry any excess energy. Even more, operating in reduced frequency, they should have less than a normal ZPE. Their operation in subharmonics will allow them to match well with the external nodes without much interaction. **The both features, lower ZPE and frequency matching in subharmonics, make the magnetic quasispheres perfect isolators of the electrical quasispheres from the external nodes.**

Accepting the condition of magnetic quasispheres as an isolators, means that they provide a boundary condition of the photonic wave. Then the transverse dimension of the wavetrain should reach a limit value (this will be discussed in the next paragraph). From the accepted case, shown in Fig. 2.37.b, we see, that we may define two types of the light velocity: one helical and one linear. They both have one and a same frequency, but are referenced to different paths. The velocity of the quantum wave propagation appears as a linear velocity, while the path of the energy momentum propagation follow helical traces. Consequently the helical light velocity should be defined for a definite radius of the wave. Following the same logic, we will distinguish two types of wavelengths for a given quantum wave: linear wavelength, referenced also as longitudinal and a helical wavelength. The use of helical wavelength is very convenient for the analysis, because it is aligned with the path of the momentum propagation. The helical wavelength should be defined for a definite radius from the central axes.

Unfolding the trace for one helical step we have: $L_h^2 = L_{lin}^2 + \pi^2 r^2$, where L_h and L_{lin} are respectively the helical and linear paths. Then the relation between the linear and helical wavelength is

$$\lambda_h = \sqrt{\lambda^2 + 4\pi^2 r^2} \qquad (2.20)$$

where: λ - is the longitudinal wavelength

We may regard the involved quasispheres, as running quasispheres with a constant light veloc-

ity. In this way we may study some of their features: **The running electrical quasisphere, appear to have energy above E_{cr2}, while the running magnetic quasisphere will have an energy equal E_{cr2}. So the photon energy is carried by the running electrical quasispheres.**

Following the above considerations we can configure the radial extent of the photon wavetrain. Fig. 2.38 illustrates this configuration in simplified way.

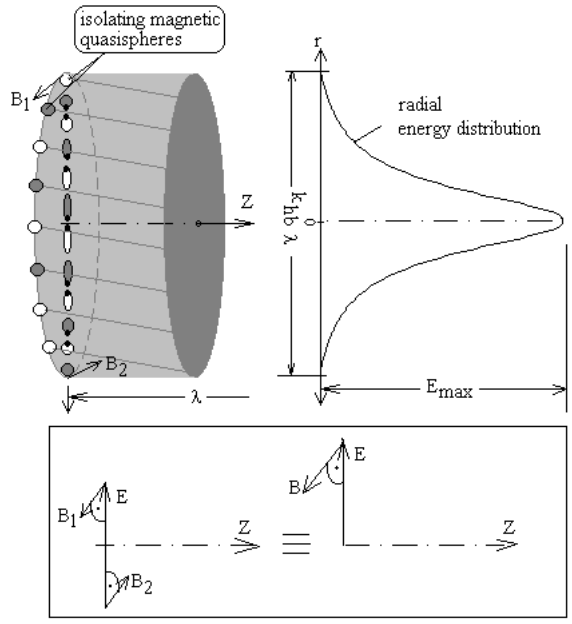

Fig. 2.38

Boundary conditions and momentum propagation

of the quantum wave

It is useful to determine the helical wavelength at the boundary radius. If accepting that the transverse wavelength is a same as the longitudinal one, then $r = \lambda/2$ and the helical path will be $\sqrt{1+\pi^2}$ times longer than the linear one. In Chapter 2, when discussing the electron, and its quantum motion, it is shown that the boundary condition become satisfied at: $r = 0.6164\lambda_o$. In §2.9.5 and §2.9.7.3 it will be shown that the transversal width is increased twice during the detection process, due to disappearing of the Coulomb forces, that keep the quantum wave integrity. So the full width of the detected wave becomes equal to 2.328. This value is pretty close to the Airy disk diameter of the monochromatic wave pattern obtained by diffraction limited optics: 2.44λ. In such case the **coefficient for the boundary conditions is:**

$$k_{hb} = \sqrt{1 + 4\pi^2(0.6164^2)} = 4 \qquad (2.20.a)$$

The above calculated value should be consistent with the boundary conditions of the quantum motion of the electron. This is discussed in Chapter 3. Despite the accepted value of 4, we will continue to use explicitly the boundary coefficient in all the equation for two reasons: to show its involvement in the equations and to give a possibility for eventual correction of its value.

The linear light velocity expressed by the path of the first harmonic is:

$$c = \frac{\lambda_o}{t_o} = \lambda_o \nu_o = \frac{\lambda_{SPM}}{t_{SPM} k_{hb}} = \frac{c_h}{k_{hb}} \qquad (2.21)$$

where: $\nu_{SPM} = \nu_o$; $t_{SPM} = t_o$

ν_o and λ_o can be called respectively: fundamental frequency and fundamental wavelength.

c - is linear velocity;

c_h - is a helical light velocity.

In Chapter 3 we will show that, in the Earth local field, the fundamental frequency and wavelength are equal respectively to the Compton frequency and Compton wavelength. So in our calculations in the next chapters we will refer this SPM parameters to the Compton's parameters, that are known with a high degree of accuracy:

$\nu_{SPM} = \nu_c$; $t_{SPM} = t_c$

Important note: While $\nu_{SPM} = \nu_c$, and $t_{SPM} = t_c$, $\lambda_{SPM} > \lambda_c$, because they are referenced to different velocities (helical and linear velocities).

In Fig. 2.38, the shape of the electrical quasisphere is shown as for not shrunk radial space. The photon is propagated in a cylindrical volume, whose boundary are defined by properly oriented peripheral magnetic quasispheres. The SPM vectors of these quasispheres operate at subharmonic of λ_{SPM}. The value of this subharmonic defines completely the photon energy. The electrical quasispheres inside the cylindrical volume have their axes normal to the axis of the wave propagation. The opposite pairs are equally deformed. The gradient of their deformation, discussed in the next paragraph, should provide an energy density simi-

lar like the Lorenzian function, with an exception of the tails. The tails fall to zero at the radius, defined by the magnetic quasispheres, due to the mentioned above transverse wavelength compact effect. The ratio between the longitudinal and transverse wavelength is a finite value, expressed by the factor k_{hb}.

It is evident from the node configuration, that the energy is carried by the central part of the wavetrain, where the deformation of the electrical quasispheres is larger. The figure 2.38 shows also the both vectors for electrical filed E and magnetic field B. The equivalent magnetic filed vector is formed of multiple distributed vectors like B_1 and B_2, that keep the rotational helical features of the photon. The vector E and distributed vectors B_1, B_2 are equivalent to two vectors E and B perpendicular each other, with common origin lying in the axis Z. By squaring the E vector we can obtain the energy in any moment. **In such case the both vectors behaves in a same way as in the wave function used in the QED** (quantum electrodynamics)**, but possessing in the same time boundary conditions**.

The photonic volume appears well isolated from the external CL space, but only for the quantum wavelength, defined by the ν_{SPM} subharmonic. For wavelengths with different quantum numbers it is transparent.

2.10.4.4. Radial energy distribution of the quantum wave

It is evident that the integrity of the photonic wave is possible if SPM vectors of all neighbouring nodes - magnetic and electric are synchronized. It has been illustrated in Fig. 2.37, that the line of synchronization of the magnetic quasispheres formes a helix centred along the axis of the wave propagation. Then the electrical nodes also must posses SPM phase synchronization along a helical trace. In the photonic wave, the degree of polarization of any EQ depends of its radial distance from Z axis.

Unfolding the helical trace of the energy propagation of one electrical node at distance r from Z axes, for time equal to t_{SPM} we have.

$$\lambda_h(r) = \sqrt{\lambda_c^2 + 4\pi^2 r^2} \qquad (2.22)$$

Dividing the trace path by the time we get the helical velocity.

$$\upsilon_h = \frac{1}{t_c}\sqrt{\lambda_c^2 + 4\pi^2 r^2} = \nu_c\sqrt{\lambda_c^2 + 4\pi^2 r^2} \qquad (2.23)$$

Eq. (2.23) provides the conditions for synchronization of the electrical quasispheres along a helical trace with radius *r*. Its plot is given in Fig. 2.39.

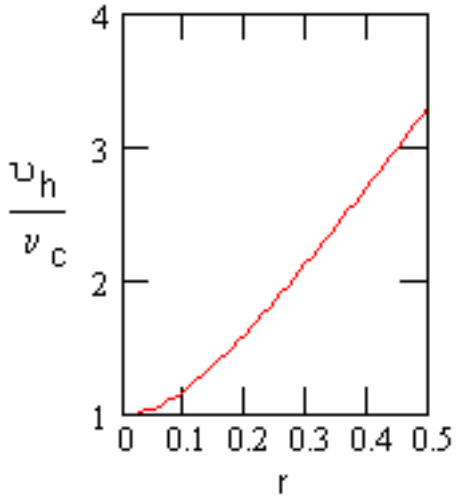

Fig. 2.39

The helical velocity at $r = 0$ approaches the value of the light velocity. This radius corresponds to the largest elongation of the electrical quasispheres. The helical light velocity is proportional to the oscillations along Z axes. The more polarised quasispheres, corresponding to smaller radius r, have less number of resonance cycles along the Z axes. Consequently the linear change of the elongation with the radius satisfies the synchronization condition according to Eq. (2.23).

According to the boundary wave conditions, the electrical quasispheres obtain minimum polarisation or practically are degenerated to magnetic quasispheres, at the boundary radius. Then the helical velocity should obtain a constant value, determined only by the harmonic number. It is logical to expect, however, that this change could not appear abruptly. It may influence also the shape of the radial velocity distribution.

We may find the shape of the radial velocity distribution by analysing the radial dependence of the propagated momentum. For this purpose we may use the photon mass equivalence for the first harmonic wave. $m_1 = h\nu/c^2$, but referenced to a single node. Then the energy dependence from the radius could be described by the equation:

$$E = \left(\frac{1}{2}\frac{m_1}{n}\frac{1}{r^x}\right)v^2 = \left(\frac{1}{2}\frac{m_1}{n}v_c^2\right)(\lambda_c^2 + 4\pi^2 r^2) \qquad (2.24)$$

where: the factor $1/r_x$ gives the radial distribution. (In the next paragraph the photon mass distribution is discussed in details).

Fig. 2.40 shows the plots of Eq. (2.24), normalized to the product $\frac{1}{2}\frac{m_1}{n}v^2$, for the following values of x: 1, 3/2, 2, 3. The horizontal scale is one and same for r and λ.

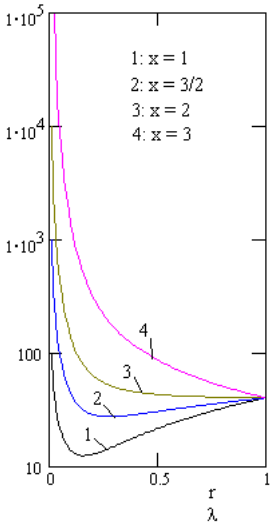

Fig. 2.40

The portion of the plots for x =1 and x=2 fall below the level of r = 05 and 1. This means too large negative energies and consequently is not acceptable. The plot for x = 3 is also not acceptable, because at radial distance of $\lambda/2$ the energy is still too high.

The plot for x = 2 only gives a reasonable energy distribution. Only this plot has a shape closer to Lorenzian shape of line. This corresponds to distribution law proportional to inverse square of the distance. It is not difficult to guess, that this is caused by the interaction forces between the positive and negative electrical quasispheres, that are Coulomb like forces. **Consequently the effect that keeps the radial integrity of the quantum wave is caused by the Coulomb forces between the positive and negative electrical quasispheres (EQs).**

Now let to make connection between the radial energy distribution and the line shape for spontaneous emission. The spectral shape of line, corresponding to a spontaneous emission is given by the Lorenzian function. Expressing the Lorenzian function by wavelength, and applying it for the first harmonic we get.

$$g(\Delta\lambda) = \frac{\delta\lambda}{2\pi c\left[\left(\frac{\Delta\lambda}{\lambda_c}\right)^2 + \left(\frac{\delta\lambda}{2\lambda_c}\right)^2\right]} \qquad (2.24)$$

where: $\Delta\lambda$ - is the wavelength change, $\delta\lambda$ is the spectral line width.

Fig. 2.40.A.a shows a plot of the radial energy distribution with the accepted inverse square law. Fig. 2.41.b gives the normalized Lorenzian line shape for different values of the spectral width, but in function of the transverse wavelength.

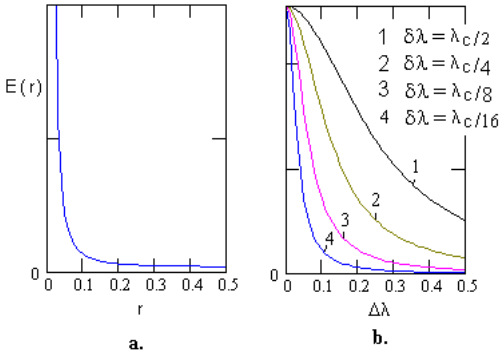

Fig. 2.40.A

Comparing the plots in Fig. 2.40.A a and b., we find that the energy distribution corresponds to a transverse width of $\lambda/16$. **This means that at distance $r = \lambda/16$, the node excess momentum falls approximately to half of its value.** Comparing to the detected line width this value appears narrower. But this line width is valid only for the quantum wave before the detection. During the detection process the Coulomb forces between EQs are destroyed and the line appears wider.

There is one important consideration about the Coulomb forces effect. The node distance should not been changed for two reasons: first one - it could affect the synchronization conditions and second one - the space occupied by a quantum wave with longer wavelength is completely transparent for a shorter wavelength quantum wave. So it appears that the Coulomb forces interaction affects the angular momentum within the resonance

cycle. This is equivalent to regarding the space of the electrical quasisphere as shrunk along its major axis. We will call this a **quasishrink effect of the lattice space**.

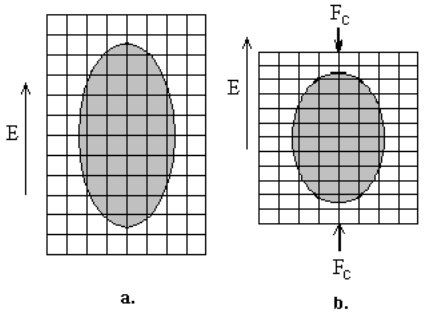

Fig. 2.40.B
Electrical quasisphere affected by a quasishrink effect of the CL space

This is illustrated graphically by Fig. 2.40.B, where: a. - shows the envelope of the quasisphere without shrinking, b. - shows the same quasisphere, shrunk by the Coulomb forces F_C.

2.10.5 Boundary conditions for the wave equation

The provided analysis about the quantum wave configuration allows to define boundary conditions for the E and H vectors, when used in the classical wave equation, for vacuum and air environment.

The radial trend of the electrical field vector E could have a shape of the curve 4 in Fig. 2.41.b, but not so sharp at the zero radius, because the EQ could obtained a finite elongation. It has to fall to zero at the boundary defined by the boundary coefficient (2.20.a). Practically, however, the EQ could not convert abruptly to MQ without some additional oscillations beyond the defined above radius. This is confirmed by the small concentric rings around the central maximum obtained by a diffraction limited optics. The oscillating energy beyond the boundary level, could not be part of the photon momentum, because its energy is independent of the path it has passed before the detection. Consequently it can be a reactive energy exchanged between the photon and the CL space. In other words it is an energy borrowed by the CL space, and used to provide zero isolation of the photon momentum. During the detection process this energy is returned back to the CL space. Practically this is possible if the slightly deformed quasispheres in the boundary domain, (whose shape is closed to MQ shape), have proper phase differences of their SPM vectors.

From the above analysis, it become evident, that when considering the energy distribution only, the E vector could be considered as dropping to zero at the boundary radius. When we are interested of the intereferometric conditions, however, the extended boundary radius for the reactive energy exchange should be considered.

The same boundary conditions are valid for the magnetic field vector H (or B), but having in mind, that it has a constant value. So, when we are interested of the energy only, the magnitude of the H vector obtains a constant value. In case of interferometric conditions it has a fluctuation component added to its constant value.

For simplified calculations, the E vector could be replaced with a constant value at the half maximum of the quantum wave.

The discussed above boundary conditions are valid for vacuum and air, but not for a transparent media as glasses. The CL space in this media is highly modulated by the EQ around the protons, that are aligned in a well defined order. The absolute frame analysis of the photon shape in this conditions is not convenient. The amazing fact, however is that the photon preserves its integrity and momentum, when passing through a homogeneous optical media. The polarization of the E vector although could be affected by the media properties, that are in fact properties of the internal CL.

2.10.6 Propagation of quasiparticle waves

Another important feature of the cosmic lattice, is that the x,y,z axes of the right handed nodes does not intercept the x,y,z axes of left handed nodes. In result of this a wave propagation only by left handed or by right handed nodes is possible.

In all cases of neutral EM waves, including the photons, the energy is emitted due to a multiple oscillations of helical particle. In this case the energy is well mixed between the right handed and left handed nodes.

In case of short and strong aperiodic oscillations, caused usually by change of the external geometry of the helical structure, the picture is different. In Chapter 6, is shown, that such kind of oscillations occurs, when the neutron transforms to a proton or vice versa. The transformation in this case is related with unlocking or locking of near field and respectively with birth or death of electrical charge. The process is also accompanied with aperioding structure motion, complimentary to a charge oscillation. The process is faster, than the CL relaxation time, so the invoked wave energy does not have a time to be equally distributed between both type of nodes. It propagates as wave exhibiting an electrical charge. We can call this type of wave a **quasiparticle wave, or virtual particle.** There are few important characteristics of this waves.

- they may reach energies, higher than the energy of the first harmonic,
- they are deflected by electrical and magnetic fields,
- their motion do not exhibit sharp quantum features like the moving electron

The first feature is possible, because the motion of this wave does not involve transmission of any intrinsic matter.

The second feature is obvious.

The third feature is explained by the difference between the quasiparticle wave and the quantum wave. While the quantum wave has an excellent isolation by the synchronized magnetic quasispheres, the quasiparticle wave does not have such one. The lack of such isolation excludes the transverse packing of the electrical charge, that is a major condition for a quantum wave formation. So the transverse radius of the wave does not have sharp boundary, but depends of the energy. The quasiparticle wave behaves as a high energy electron or positron. In the process known as a positron moderation, the positive quasiparticle wave interacts with an electron, in result of which, a low energy real positron particle is extracted. (see Chapter 6).

The quasiparticle waves, perhaps propagates with a light velocity, but the BSM theory does not have enough experimental data about such conclusion.

The lack of quantum effect means a lack of synchronization of the running MQ's involved in the wave volume. But why such synchronization is missing? The neutral quantum wave has one important feature: the neighbouring positive and negative (left and right handed) quasispheres have complimetary interaction of their resonance momentums. The complimentary interaction is supported by the carried energy momentum. In the quasiparticle wave, such interaction are missing. If the wave is a positive, for example, every neighbouring quasisphere is a magnetic, and not synchronized to it's neighbour EQ's. In such way, the amount of the not synchronised magnetic quasispheres in the volume is quite large in comparison to the neutral wave. Then a formation of boundary magnetic quasispheres, synchronized to external SPM frequency is not possible. The strong quantum effect defined by the external boundary conditions is disturbed.

One question arises: How the integrity of the quasiparticle wave is kept? The possible explanation is the following.

The EQ eccentricity in the wave cross section has a radial dependence. If assuming, that it is similar as in the stationary E-filed of the electron (see Chapter 3), it is higher in some intermediate radius value. This is illustrated in Fig. 2.41.A, where **a.**

shows the radial E field of the electron and **b**. shows the radial E field of a quasiparticle wave.

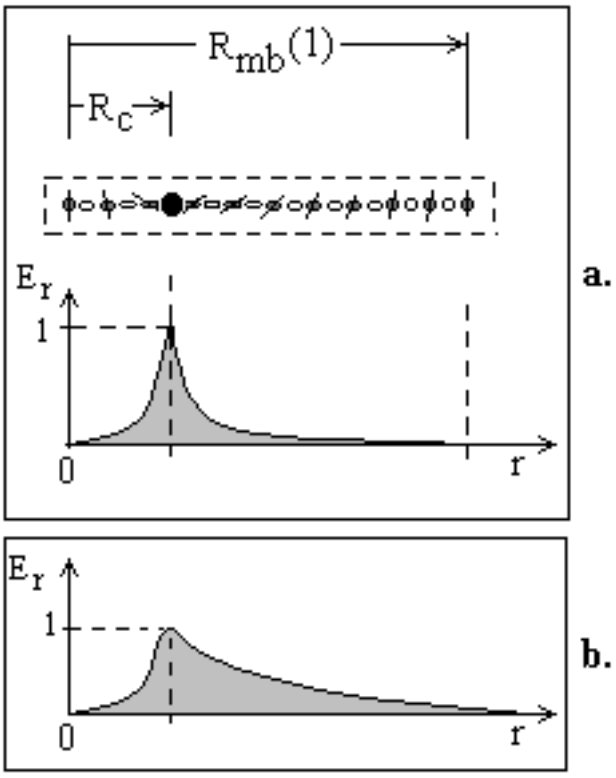

Fig. 2.41.A

When the radius approaches zero, the E-field also tends to zero. This is reasonable for the electron. From the interaction between the electron and quasiparticle waves leading to emission of gamma wave or extraction of the internal positron, we may conclude that the quasiparticle wave has a similar configuration. In such case the central axis zone of the quasiparticle wave should be occupied by MQ's. Then they could be synchronised by SPM frequency. So the quasiparticle wave may have a central core of MQ's synchronised to the Compton frequency. This core could keep the integrity of the wave. It could serve as a quantum feature, assuring in the same time motion of the wave with a light velocity. This feature may appear as an energy modulation condition for waves with different energies. Despite the relative weakness of this quantum feature, it may play a role for the wave integrity. A signature of such feature appears in the spectra of the quasiparticle waves, obtained from a β radioactive decay. Fig 2.41.B, shows spectra of β "particles" from decay of ^{64}Cu.

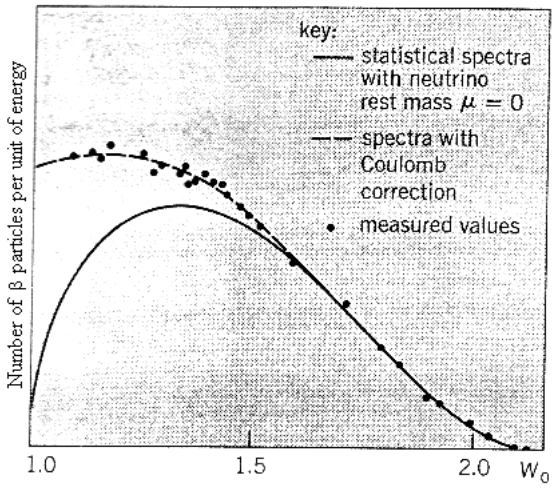

Fig. 2.41.B

Spectra of β decay of ^{64}Cu. The quantity W is the total beta-particle energy in the units of the electron rest energy. (C. P. Parker, 1993), courtesy of L. M. Langer et al., 1949)

From the analogy between the quasiparticle wave with the electron we see, that it's radial configuration is different than the neutral quantum wave. From the spectral plot in Fig. 2.41.B we also see, that the limit value of the negative QP wave approaches a quantum feature of energy modulation at 2.1 MeV. It is approximately 4 time the energy of the neutral first quantum wave (energy of the electron). This may lead to guess about the possible radial configuration of the QP wave. The possible configuration is presented in Fig. 2.41.C by Eq's, where case a. is for a neutral quantum wave and case b. - for a QP wave.

Fig. 2.41.C

Fig. 2.41.C (a) shows a wavetrain cross section of a neutral quantum wave of first harmonics where the E-field vector is shown as aligned EQs of both type. Fig. 2.41.C. (b) shows the possible arrangement of EQs for a case of quasiparticle wave. In this case only one type of aligned EQs exists and the boundary conditions are absent. But the arrangement of the EQs are not like in the neutral first harmonic wave, but as in the E-field of the electron shown in Fig. 2.41. In such the internal core of aligned MQ's in the centre may assure a quantum feature at SPM wavelength, that could allow keeping of the charge integrity. But this integrity may exist only if the wavelike structure is moving with the speed of light. The IG conditions that keep the charge unity however are missing, so this quasiparticle structure is most probably to absorbed at once. The absence of boundary conditions also does not put a limit on the limit the radial extent. So we may accept that the structure shown in Fig. 2.41.C (b) (one diameters of aligned EQ of same type) carry an energy of 511 KeV. Then a second arrangement of similar structure with two diametrical EQ alignment at 90 deg should carry energy of $2 \times 0.511 = 1.022 \text{ MeV}$. The right angle between the two cords might be and optimal arrangement corresponding to the observed maximum in Beta decay illustrated by Fig. 2.41.B. The cut-off about 2 MeV may corresponds to four diametrical arrangements $4 \times 0.511 = 2.044 \text{ MeV}$. The continuum of the Beta spectra could be explain with the feature that the charge unity is not preserved (missing IG field as in the static charge). Some continuously decrease of the electrical charge may give effect of electron moving with different velocities.

Quasiparticle waves are emitted in the radioactive decays, where the proton-neutron (and neutron-proton) conversions are involved. Additional discussion about the process of their generation is presented in Chapter 6.

2.10.7. Gamma rays as a bunch of quantum waves

From the two basic conditions for the boundary conditions and the integrity of the quantum wave, it follows, that the SPM frequency of the CL space puts an upper limit for the wavelength (and frequency) of the quantum wave. Then quantum wave with shorter wavelength than the λ_{SP} could not exist. This means, that the quantum wave configuration described so far is valid for the subharmonics of SPM frequency (including the first one), but not for harmonics. But how to explain the gamma photon, whose energy can be below and above the energy of the first harmonic quantum wave? The only possible configuration of the gamma photon is to be an entagled packet of SPM quantum waves.

The photon entaglement is proved to exist in the light produced by the lasers. The physical shape of the entagled photon could be inferred from the point of view of BSM considerations. The entagled photons could be consisted of two and more quantum waves.

Let to consider initially photon energy below the energy of the first harmonic. We may distinguish two types of entagled photons: parallel and serial. The serial entagled photons should be exactly with the same subharmonic number. The parallel entagled photons, when their number is above two, may contain photons with different quantum numbers. Let pay attention especially on the last case. The physical conditions allowing the entaglement obviously are related with the keeping of the photon energy in compact space, that however is not stationary but moving with the light velocity. But for the stationary nodes this means a reduced interaction between the surrounding CL space and the photon space. The only possible way for this is to reduce the common boundary surface between the entagled photon and the surrounding space. According to these considerations, the possible configuration of the parallel entagled photon is a

"rope" like structure. Such configuration is shown in Fig 2.42.

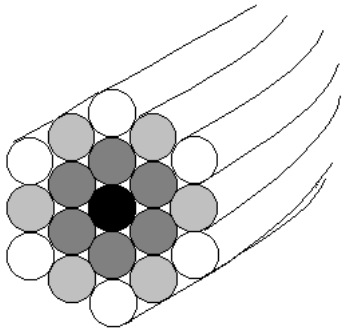

Fig. 2.42
Cross section of parallel entagled photon structure

From the shown configuration, we see, that the boundary structure if the entagled photon is smaller that the sum of the boundary structures of the individual photons. In the real case the individual circles in the cross section could be slightly separated. In such case the individual boundary conditions still could be satisfied, due to the reactive energy exchange, that was mentioned in §.2.10.5.

The parallel entagled photon could include individual photons with different wavelength. In this case, they are twisted around the central core wavelength. This gives to the entagled photon not only compactness but additional stiffness. So they are difficult to be separated. The photon included in the centre of the structure is with the shortest wavelength. This is the core photon of the entagled structure. The core photon in the structure, shown in Fig. 2.42 is shaded black. The surrounding photons whose centre in the cross section is peripheral in respect to the central one posses larger wavelengths. The wavetrain cross sections of the photons with the same wavelengths, shown in Fig. 2.42 are shaded with a same gray level. The common wavetrain structure could be regarded as a group.

The configuration shown in Fig. 2.42 does not cover the diversity of the entagled photons. The wavetrain length of the short wavelength photons from the first harmonic to the near infrared range is much longer, than their wavelength The entagled photons are proved to exists in the laser light in the VIS and near IR range. According to BSM analysis, the photons in the ultra shot laser pulses (known as "femtosecond pulses") contain large number of parallel entagled photons. So if entagled photons are able to exists in the visible and near IR range, they are even more likely to exist in the range near to the Compton wavelength.

Let introduce an index of "basic order" corresponding to the number of radii passing through the centre of the wavetrain with equal wavelength. The basic order number of the configuration shown in Fig. 2.42 is 3. Let suppose, that the basic order number reaches sum limit, that is intrinsic of the CL space. The group in such case is completed. Then it could be possible to get a second order bunch comprised of such groups in a similar way, as the individual photons of the group. We may use the index "group order" in a similar way as the "basic order" The total energy of such entagled photon will be a sum of the energy of all contained individual photons. If the energy of the entagled photon is much larger than the first harmonic, the photon structure could be a parallel entagled photon containing bunches of groups. Now we arrive to the possible configuration of the high energy gamma photon.

It is obvious, that the connection between the individual wavetrains within the group is stronger, than the connection between the groups, due to the different interspaces in the radial section. Then a parallel entagled photon of group order higher than one will exhibit one specific feature. The groups may be displaced along the wavetrain length. This displacement could be influenced by the CL relaxation time. Then the phase of the entagled photon regarded as a pulse of light could exhibit curled features in the front and back ends. Such features are observed in the ultra short laser pulses in the near IR region,. Such pulses are achromatic. Their specific features show that parallel entagled photons are possible also in the much shorter quantum waves. This is one indirect indication that the gamma quant is a bunch of entagled photons.

We may summarize:

- **The gamma quant is a bunch of parallel entagled quantum waves, arranged in groups.**

- **The gamma quant is achromatic, comprised by individual photons that are harmonics and subharmonics of the SPM frequency.**
- **For high energy gamma quant, the central photon of any one of the group is a first harmonic wave.**
- **The lower energy gamma may contain only one group and the central photon may be a subharmonic of the SPM frequency**

2.10.8 Trapping mechanism of rectangular lattice inside the helical structures.

When a first order helical structure does not contain internal structure its modified rectangular lattice forms an axial trapping hole. Such configuration was discussed in §2.6.5 This type of lattice does not possesses SPM effect, and consequently does not propagate a magnetic field. The radial stripes, however are excellent propagator of the IG TP field of the helical shell. So we may consider, that the electrical field of this shell is propagated without losses and focused on the central hole. If the first order helical structure is built by right handed prisms, a node of left handed prism aligned to the axis will be attracted, then folded into a core of four prisms and trapped by the hole. If number of such nodes are folded and trapped, they will be connected together, forming a straight core structure, consisting of one central and six peripheral prisms. So we see, that the CL folded nodes can built a long core, that is not distinguished from the core the helical structures are built of.

The process of prism to prism interaction in the hole is enhanced due to two factors: 1) The gravitation of the central part of the trapping whole serves only to align the prism. Therefore the trapped node of prisms appears weightless in the centre of the hole, and only the twisted part interaction is effective. 2) The lattice configuration provides a focusing of the helical core handedness into the space of the trapping hole. This enhance the peripheral interaction between the focused IG field and the trapped prisms, of the folded node.

According to BSM theory the trapping mechanism shows its signature in some of the processes in the particle coliders. The regeneration of K_o^L from K_o^S, for example, known as a CPT violation, is explained by BSM theory as a central core generation by the trapping mechanism. This is discussed in Chapter 6.

The trapping mechanism is important effect, helping to explain some of the processes during the phase of particle crystallization. This phase precedes the birth of the galaxy.